Electronic Supplementary Material (ESI) for Dalton Transactions.

Supporting Information

Insights into the antiproliferative mechanism of (C^N)-chelated half-sandwich iridium complexes

Robin Ramos, Jérémy M. Zimbron, Serge Thorimbert, Lise-Marie Chamoreau, Annie Munier, Candice Botuha, Anthi Karaiskou, Michèle Salmain* and Joëlle Sobczak-Thépot*

Abstract: Transition metal-based anticancer compounds, as alternative to platinum derivatives, are raising scientific interest as they may present distinct although poorly understood mechanisms of action. We used a structure-activity relationship-based methodology to investigate the chemical and biological features of a series of ten (C^N)-chelated half-sandwich iridium^{III} complexes of the general formula [IrCp*(phox)Cl], where (phox) is a 2-phenyloxazoline ligand forming a 5-membered metallacycle. This series of compounds undergoes a fast exchange of their chlorido ligand once solubilised in DMSO. They were cytotoxic to HeLa cells with IC_{50} values in the micromolar range and induced a rapid activation of caspase-3, an apoptosis marker. *In vitro*, the oxidative power of all the complexes towards NADH was highlighted but only the complexes bearing substituents on the oxazoline ring were able to produce H_2O_2 at the micromolar range. However, we demonstrated using a powerful HyPer protein redox sensor-based flow cytometry assay that most complexes rapidly raised intracellular levels of H_2O_2. Hence, this study shows that oxidative stress can partly explain the cytotoxicity of these complexes on the HeLa cell line and gives a first entry to their mechanism of action.

Table of Contents

Materials, methods and instrumentation

Synthetic procedures and characterization

Compounds **L1-L4**, **L6**, **L8-L10** are commercially available but all synthesized compounds are herein fully described. **L7** was reported in literature[1] without synthetic description nor characterization. **Ir1**[2], **Ir2**[3], **Ir8**[4] were previously reported in the literature. Reagents were purchased as reagent-grade and used without further purification. All reactions were performed under nitrogen atmosphere, were monitored by analytical TLC on silica gel 60 F254 plates 0.25 mm, and visualized under UV light (λ = 254 and 354 nm). Silica gel (SDS 60 ACC 35–70 mm) was used for column chromatography. NMR spectra were recorded on Bruker Avance III 300 MHz or 400 MHz spectrometers at room temperature. Chemical shifts (δ) are expressed in part per million (ppm), reported as s = singlet, d = doublet, t = triplet, m = multiplet; and referenced to the solvent peak of respectively $CDCl_3$, CD_2Cl_2, $(CD_3)_2SO$ (^{13}C NMR: δ = 77.23; 53.84; 39.52 ppm; ^1H NMR: δ = 7.26; 5.32; 2.50 ppm). Optical rotation measurement of **L7** was performed with a Jasco P-200 digital polarimeter.

General procedure A, 2-phenyl-4,5-dihydrooxazoles L2-L4 and L7-L10: At room temperature, ß-amino alcohol (2.5 eq) was added slowly to a solution of aroyl chloride in dichloromethane (1.0 eq, 0.5 M). The reaction mixture was stirred at room temperature for 1 to 16 h. The whole mixture was transferred in a separating funnel containing water. The organic layer was discarded and the aqueous layer was extracted with EtOAc. The combined organic layers were dried over magnesium sulfate, filtered and concentrated in vacuo to afford the corresponding ß-arylamide alcohol. At room temperature, $SOCl_2$ (4.0 eq) was added dropwise to a solution of ß-arylamide alcohol in dichloromethane (1.0 eq, 0.1 M). The reaction mixture was stirred overnight at room temperature. The mixture was poured into ice water/EtOAc (1:1), and neutralized to pH = 6-8 by adding solid $NaHCO_3$. The whole mixture was transferred in a separating funnel and the aqueous layer was extracted with EtOAc. The combined organic layers were dried over magnesium sulfate, filtered and concentrated in vacuo. The crude product was purified by silica gel column chromatography using cyclohexane (Cy) and ethyl acetate (EtOAc) to afford the corresponding 2-phenyl-4,5-dihydrooxazoles **L** as a pure product.

General procedure B, 2-phenyl-4,5-dihydrooxazoles L5 and L6: Using deactivated aroyl chloride (4-nitro-benzoylchloride and 4-(chloromethyl)benzoyl chloride) and ß-amino alcohol, procedure A afforded the corresponding intermediate ß-arylamide chloride as a crude product. Without purification, the crude ß-arylamide chloride was dissolved in dry THF (1.0 eq, 0.2 M) and NaH (60% in oil, 1.5 eq) was slowly added at room temperature. The reaction was stirred for 1 h and quenched by adding sat. aq. NH_4Cl solution. The whole mixture was transferred in a separating funnel. The organic layer was discarded and the aqueous layer was extracted twice with EtOAc. The combined organic layers were dried over magnesium sulfate, filtered and concentrated in vacuo to afford the expected 2-phenyl-4,5-dihydrooxazole as a pure product.

L2: 4,4-dimethyl-2-phenyl-4,5-dihydrooxazole

Obtained following procedure A as a colorless oil, purified using Cy/EtOAc (8:2) to yield 65%

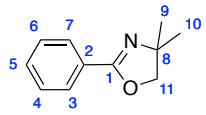

^1H NMR (300 MHz, $CDCl_3$) δ (ppm): 7.95 (d, 2H, *J* = 6.7 Hz, $H_{3,7}$), 7.51-7.35 (m, 3H, $H_{4,5,6}$), 4.12 (s, 2H, H_{11}), 1.39 (s, 6H, $H_{9,10}$). **^{13}C {^1H} NMR** (75 MHz, CD_2Cl_2) δ (ppm): 162.03 (C_1), 131.12 (C_5), 128.24 ($C_{4/6}$), 128.20 ($C_{4/6}$), 128.08 (C_2), 79.11 (C_{11}), 67.56 (C_8), 28.41 ($C_{9,10}$). **HRMS** (ESI+): *m/z* calculated for $C_{12}H_{15}NONa$: 198.0889; found: 198.0889 $[M+Na]^+$.

L3: 2-(4-fluorophenyl)-4,5-dihydrooxazole

Obtained following procedure A as pale pink crystals, purified using Cy/EtOAc (5:5) to yield 41%

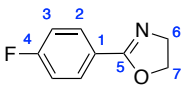

^1H NMR (300 MHz, $CDCl_3$) δ (ppm): 8.01 (ddd, 2H, *J* = 8.9, 5.2, 2.4 Hz, H_2), 7.12 (m, 2H, H_3), 4.49 (t, 2H, *J* = 9.6 Hz, H_7), 4.09 (t, 2H, *J* = 9.5 Hz, H_6). **^{13}C {^1H} NMR** (75 MHz, $CDCl_3$) δ (ppm): 166.34-163.01 (C_4, *J* = 251.7 Hz), 163.82 (C_5), 130.48-130.36 (C_2, *J* = 8.9 Hz), 123.90 (C_1), 115.61-115.32 (C_3, *J* = 22 Hz), 67.79 (C_7), 54.81 (C_6). **HRMS** (ESI+): *m/z* calculated for C_9H_9FNO: 166.0663; found: 166.0661 $[M+H]^+$.

L4: 2-(4-methoxyphenyl)-4,5-dihydrooxazole

Obtained following procedure A as pink crystals, purified using 100% Cy to Cy/EtOAc (5:5 +1% Et_3N) to yield 52%

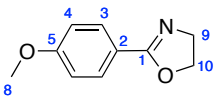

^1H NMR (300 MHz, $CDCl_3$) δ (ppm): 7.90 (d, 2H, *J* = 8.8 Hz, H_3), 6.92 (d, 2H, *J* = 8.8 Hz, H_4), 4.42 (t, 2H, *J* = 9.5 Hz, H_{10}), 4.04 (t, 2H, *J* = 9.3 Hz, H_9), 3.86 (s, 3H, H_8). **^{13}C {^1H} NMR** (75 MHz, $CDCl_3$) δ (ppm): 164.37 (C_1), 161.97 (C_5), 129.81 (C_3), 120.27 (C_2), 113.62 (C_4), 67.44 (C_{10}), 55.28 (C_8), 54.82 (C_9). **HRMS** (ESI+): *m/z* calculated for $C_{10}H_{12}NO_2$: 178.0863; found: 178.0860 $[M+H]^+$.

L5: 2-(4-nitrophenyl)-4,5-dihydrooxazole

Obtained following procedure B as a yellow solid, 75%

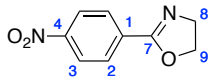

^{1}H NMR (300 MHz, $CDCl_3$) δ (ppm): 8.29 (m, 2H, H_2), 8.14 (m, 2H, H_3), 4.52 (t, 2H, *J* = 9.5 Hz, H_9), 4.15 (t, 2H, *J* = 9.5 Hz, H_8). **^{13}C {^{1}H} NMR** (75 MHz, $CDCl_3$) δ (ppm): 162.87(C_7), 133.52(C_4), 129.17(C_2), 123.52(C_3), 68.14(C_9), 55.24(C_8). **HRMS** (ESI+): *m/z* calculated for $C_{10}H_{12}NO_2$: 193.0608; found: 193.0608 $[M+H]^+$.

L6: 2-(4-(chloromethyl)phenyl)-4,5-dihydrooxazole

Obtained following procedure B as a yellow solid, 99%

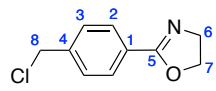

^{1}H NMR (400 MHz, $CDCl_3$) δ (ppm): 7.94 (d, 2H, *J* = 8.2 Hz, H_3), 7.43 (d, 2H, *J* = 8.2 Hz, H_2), 4.61 (s, 2H, H_8), 4.44 (t, 2H, *J* = 9.5 Hz, H_7), 4.07 (t, 2H, *J* = 9.5 Hz, H_6). **^{13}C {^{1}H} NMR** (75 MHz, $CDCl_3$) δ (ppm): 164.28(C_5), 140.64(C_4), 128.71(C_3), 128.63(C_2), 127.97(C_1), 67.83(C_7), 55.15(C_6), 45.76(C_8).

L7: *(R)*-4-isopropyl-2-phenyl-4,5-dihydrooxazole

Obtained following procedure A as a yellow oil, purified using Cy/EtOAc (95:5) to yield 74%

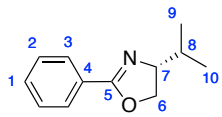

^{1}H NMR (300 MHz, $CDCl_3$) δ (ppm): 7.98(dt, 2H, *J* = 6.9, 1.5 Hz, H_3), 7.44(m, 3H, $H_{1,2}$), 4.43(m, 1H, H_7), 4.15 (m, 2H, H_6), 1.89 (m, 1H, H_8), 1.05(d, 3H, *J* = 6.8 Hz, $H_{9/10}$), 0.95(d, 3H, *J* = 6.8 Hz, $H_{9/10}$). **^{13}C {^{1}H} NMR** (75 MHz, $CDCl_3$) δ (ppm): 163.39(C_5), 131.18(C_1), 128.25($C_{2,3}$), 127.87(C_4), 72.51(C_6), 70.09(C_7), 32.80(C_8), 18.93($C_{9/10}$), 18.04($C_{9/10}$). **HRMS** (ESI+): *m/z* calculated for $C_{12}H_{16}NO$: 190.1226; found: 190.1227 $[M+H]^+$. **$[\alpha]^{22}_D$** = +81.651° (c 0.63, $CHCl_3$)

L8: *(S)*-4-isopropyl-2-phenyl-4,5-dihydrooxazole

Obtained following procedure A as a yellow oil, purified using Cy/EtOAc (9:1) to yield 74%

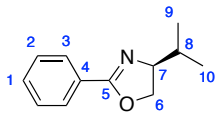

^{1}H NMR (300 MHz, DMSO-d_6) δ (ppm): 7.88 (m, 2H, H_3), 7.55 (m, 1H, H_1), 7.47 (m, 2H, H_2) 4.43 (m, 1H, H_7), 4.10 (m, 2H, H_6), 1.75 (m, 1H, H_8), 0.96 (d, 3H, *J* = 6.6 Hz, $H_{9/10}$), 0.88 (d, 3H, *J* = 6.6 Hz, $H_{9/10}$). **^{13}C {^{1}H} NMR** (75 MHz, DMSO-d_6) δ (ppm): 162.34(C_5), 131.70(C_1), 128.92(C_3), 128.20(C_2), 128.05(C_4), 72.39(C_6), 70.28(C_7), 32.83(C_8), 19.03($C_{9/10}$), 18.63($C_{9/10}$).

L9: (*R*)-2,4-diphenyl-4,5-dihydrooxazole

Obtained following procedure A as a pale orange solid, purified using Cy/EtOAc (9:1) to yield 66%

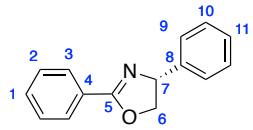

^{1}H NMR (300 MHz, DMSO-d_6) δ (ppm): 7.97 (m, 2H, H_3), 7.60 (t, 1H, *J* = 7.2 Hz, H_1), 7.52 (m, 2H, H_2), 7.38 (m, 2H, H_9), 7.32 (m, 3H, $H_{10,11}$), 5.42 (dd, 1H, *J* = 10.0, 8.1 Hz, H_6), 4.85 (dd, 1H, *J* = 10.1, 8.5 Hz, H_6), 4.21 (t, 1H, *J* = 8.3 Hz, H_7). **^{13}C {^{1}H} NMR** (75 MHz, DMSO-d_6) δ (ppm): 163.71(C_5), 143.12(C_4), 132.12, 129.10, 129.00, 128.45, 127.76, 127.10, 74.86(C_6), 69.56(C_7).

L10: (*S*)-2,4-diphenyl-4,5-dihydrooxazole

Obtained following procedure A as an orange solid, purified using Cy/EtOAc (9:1) to yield 49%

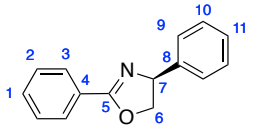

^{1}H NMR (300 MHz, DMSO-d_6) δ (ppm): 7.97 (m, 2H, H_3), 7.60 (t, 1H, *J* = 7.2 Hz, H_1), 7.52 (m, 2H, H_2), 7.38 (m, 2H, H_9), 7.32 (m, 3H, $H_{10,11}$), 5.42 (dd, 1H, *J* = 10.0, 8.1 Hz, H_6), 4.85 (dd, 1H, *J* = 10.1, 8.5 Hz, H_6), 4.21 (t, 1H, *J* = 8.3 Hz, H_7). **^{13}C {^{1}H} NMR** (75 MHz, DMSO-d_6) δ (ppm): 163.71(C_5), 143.12(C_4), 132.12, 129.10, 129.00, 128.45, 127.76, 127.10, 74.86(C_6), 69.56(C_7). **HRMS** (ESI+): *m/z* calculated for $C_{15}H_{14}NO$: 224.1070; found: 224.1068 $[M+H]^+$.

General procedure C used for the complexation of the ligands[4]: To a solution of 2-phenyl-4,5-dihydrooxazole in CH_2Cl_2 (2.2 eq, 0.02 M), were added $[Cp^*IrCl_2]_2$ (1.0 eq) and NaOAc (6.0 eq). The reaction mixture was stirred 1 to 2 days at room temperature. Then, the reaction mixture was filtered over a pad of celite, the resulting filtrate was concentrated to dryness in vacuo to afford the crude product. Purification was then carried out using silica gel column chromatography (indicated eluent) or recrystallization.

Ir1: Chlorido(η^5-pentamethylcyclopentadienyl)(2-(phenyl-κC^2)-4,5-dihydrooxazole-κN)Iridium (III)

Obtained following procedure C as a yellow powder, purified using CH_2Cl_2/EtOAc (9:1) to yield 82%, crystallized from MeOH/hexane

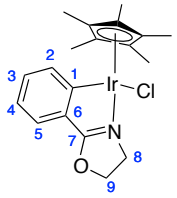

^{1}H NMR (400 MHz, CD_2Cl_2) δ (ppm): 7.77 (d, 1H, *J* = 7.5 Hz, H_2), 7.38 (dd, 1H, *J* = 7.5, 0.9 Hz, H_5), 7.20 (td, 1H, *J* = 7.5, 1.3 Hz, H_3), 6.99 (td, 1H, *J* = 7.5, 1.1 Hz, H_4), 4.88 – 4.76 (m, 2H, H_9), 3.96 – 3.87 (m, 2H, H_{10}), 1.75 (s, 15H, H^{Cp^*}). **^{13}C {^{1}H} NMR** (75 MHz, $CDCl_3$) δ (ppm): 180.30 (C_1), 164.10 (C_7), 135.65 (C^{Ar}), 132.36 (C^{Ar}), 130.71 (C_6), 126.45 (C^{Ar}), 121.79 (C^{Ar}), 87.69 (C^{Cp^*}), 71.40 (C_9), 50.38 (C_8), 9.48 ($CH_3^{Cp^*}$). **HRMS** (ESI+): *m/z* calculated for $C_{19}H_{23}IrNO$: 474.1404; found: 474.1400 $[M\text{-}Cl]^+$.

Ir2: Chlorido(η^5-pentamethylcyclopentadienyl)(2-(4,4-dimethylphenyl-κC^2)-4,5-dihydrooxazole-κN)Iridium (III)

Obtained following procedure C as an orange oil, purified using Cy/EtOAc (8:2) to yield 76%

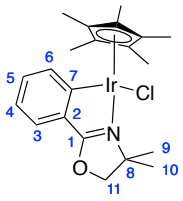

^{1}H NMR (400 MHz, CD_2Cl_2) δ (ppm): 7.74 (d, 1H, *J* = 7.7 Hz, H_6), 7.38 (d, 1H, *J* = 7.5 Hz, H_3), 7.21 (td, 1H, J = 7.5, 1.3 Hz, H_5), 6.98 (t, 1H, *J* = 7.3 Hz, H_4), 4.54 (d, 1H, *J* = 8.2 Hz, H_{11a}), 4.39 (d, 1H, *J* = 8.2 Hz, H_{11b}), 1.75 (s, 15H, H^{Cp^*}), 1.47 (s, 6H, $H_{9,10}$).**^{13}C {^{1}H} NMR** (75 MHz, $CDCl_3$) δ (ppm): 177.91 (C_7), 162.57 (C_1), 135.11 (C^{Ar}), 132.05 (C^{Ar}), 132.00 (C_2), 126.23 (C^{Ar}), 121.59 (C^{Ar}), 87.80 (C^{Cp^*}), 82.71 (C_{11}), 67.27 (C_8), 28.61($C_{9/10}$), 26.27 ($C_{9/10}$), 9.92 ($CH_3^{Cp^*}$). **HRMS** (ESI+): *m/z* calculated for $C_{21}H_{27}IrNO$: 502.1717; found: 502.1701 $[M\text{-}Cl]^+$.

Ir3: Chlorido(η^5-pentamethylcyclopentadienyl)(2-(4-fluorophenyl-κC^2)-4,5-dihydrooxazole-κN)Iridium (III)

Obtained following procedure C as a yellow powder, purified using CH_2Cl_2/EtOAc (95:5) to yield 38%

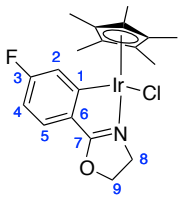

^{1}H NMR (300 MHz, $CDCl_3$) δ (ppm): 7.46 (m, 2H, $H_{2,4}$), 6.71 (m, 1H, H_5), 4.84 (m, 2H, H_9), 4.04 (m, 2H, H_8), 1.79 (s, 15H, H^{Cp^*}). **^{13}C {^{1}H} NMR** (75 MHz, $CDCl_3$) δ (ppm): 179.24(C_1), 167.09-167.02(C_7, *J* = 5.9 Hz), 166.86-163.48(C_3, *J* = 256 Hz), 128.31-128.18 (C_5, *J* = 9.6 Hz), 126.88-128.89(C_6, *J* = 1.4 Hz), 121.71-121.48(C_2, *J* = 17.7 Hz), 109.39-109.07(C_4, *J* = 23.8 Hz), 87.76(C^{Cp^*}), 71.39(C_9), 50.24(C_8), 9.33($CH_3^{Cp^*}$). **HRMS** (ESI+): *m/z* calculated for $C_{19}H_{22}FIrNO$: 492.1309; found: 492.1297 $[M\text{-}Cl]^+$.

Ir4: Chlorido(η^5-pentamethylcyclopentadienyl)(2-(4-methoxyphenyl-κC^2)-4,5-dihydrooxazole-κN)Iridium (III)

Obtained following procedure C as an orange solid, purified using recrystallization (hexane) to yield 69%

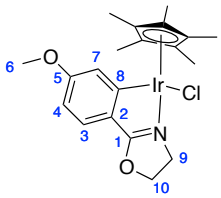

^{1}H NMR (300 MHz, $CDCl_3$) δ (ppm): 7.35 (d, 1H, *J* = 8.4 Hz, H_3), 7.32 (d, 1H, *J* = 2.0 Hz, H_7), 6.53 (dd, 1H, J = 8.2, 2.0 Hz, H_4), 4.81-4.72 (m, 2H, H_{10}), 4.09-3.91 (m, 2H, H_9), 3.86 (s, 3H, H_6), 1.76 (s, 15H, H^{Cp^*}). **^{13}C {^{1}H} NMR** (75 MHz, $CDCl_3$) δ (ppm): 179.35 (C_8), 165.86, 162.22, 127.57, 123.50, 120.00, 107.87, 87.35 ($CH_3^{Cp^*}$), 71.11 (C_{10}), 54.81 (C_6), 49.94 (C_9), 9.19 (C^{Cp^*}). **HRMS** (ESI+): *m/z* calculated for $C_{20}H_{25}IrNO_2$: 504.1510; found: 504.1530 $[M\text{-}Cl]^+$.

Ir5: Chlorido(η^5-pentamethylcyclopentadienyl)(2-(4-nitrophenyl-κC^2)-4,5-dihydrooxazole-κN)Iridium (III)

Obtained following procedure C as a brick red solid, purified using Cy/EtOAc (5:5) to yield 61%

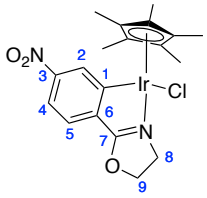

^{1}H NMR (300 MHz, $CDCl_3$) δ (ppm): 8.59 (s, 1H, H_2), 7.85 (d, 1H, *J* = 8.3 Hz, H_5), 7.52 (d, 1H, *J* = 8.3 Hz, H_4), 4.90 (m, 1H, H_9), 4.08 (m, 1H, H_8), 1.80 (s, 15H, H^{Cp^*}). **^{13}C {^{1}H} NMR** (101 MHz, $CDCl_3$) δ (ppm): 179.24(C_1), 165.27(C_7), 149.74(C_3), 136.73(C_6), 129.71(C_2), 126.88($C_{4/5}$), 117.37($C_{4/5}$), 88.61(C^{Cp^*}), 71.93(C_9), 50.84(C_8), 9.53($CH_3^{Cp^*}$). **HRMS** (ESI+): *m/z* calculated for $C_{19}H_{23}ClIrN_2O_3$: 519.1255; found: 519.1269 $[M+H]^+$.

Ir6: Chlorido(η^5-pentamethylcyclopentadienyl)(2-((4-chloromethyl)phenyl-κC^2)-4,5-dihydrooxazole-κN)Iridium (III)

Obtained following procedure C as a pale yellow solid, purified recrystallization (acetone/pentane) to yield 57%

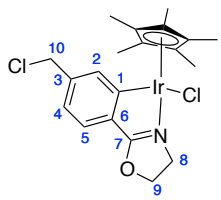

^{1}H NMR (400 MHz, CD_2Cl_2) δ (ppm): 7.78 (s, 1H, H_2), 7.38 (d, 1H, *J* = 7.8 Hz, H_5), 7.03 (dd, 1H, *J* = 7.8, 1.6 Hz, H_4), 4.83 (m, 2H, H_9), 4.72 (d, 1H, *J* = 11.5 Hz, H_{10a}), 4.63 (d, 1H, *J* = 11.4 Hz, H_{10b}), 4.09 (ddd, 1H, *J* = 12.4, 9.9, 7.6 Hz, H_{8a}), 3.91 (ddd, *J* = 12.3, 10.4, 9.1 Hz, H_{8b}), 1.76 (s, 15H, H^{Cp^*}). **^{13}C {^{1}H} NMR** (101 MHz, CD_2Cl_2) δ (ppm): 180.04(C_1), 165.22(C_7), 141.14(C_3), 136.27(C_2), 131.77(C_6), 126.62(C_4), 122.53(C_5), 88.41(C^{Cp^*}), 72.27(C_9), 50.90(C_8), 47.46(C_{10}), 9.66($CH_3^{Cp^*}$). **HRMS** (ESI+): *m/z* calculated for $C_{20}H_{24}IrNO$: 522.1170; found: 522.1160 $[M\text{-}Cl]^+$.

Ir7: Chlorido(η^5-pentamethylcyclopentadienyl)((*R*)-4-isopropyl-2-(phenyl-κC^2)-4,5-dihydrooxazole-κN)Iridium (III)
Obtained following procedure C as a yellow solid, purified using Cy/EtOAc (8:2) to yield 83%

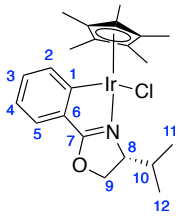

(2 diastereomers 1:0.1)
^{1}H NMR (400 MHz, $CDCl_3$) δ (ppm): 7.73 (d, 1H, *J* = 7.3 Hz, H_5), 7.36 (dd, 1H, *J* = 7.5, 1.0 Hz, H_2), 7.20 (td, 1H, *J* = 7.5, 1.5 Hz, H_3), 6.97 (td, 1H, *J* = 7.4, 1.0 Hz, H_4), 4.71 (m, 1H, H_{9a}), 4.63 (t, 1H, *J* = 9.3 Hz, H_{9b}), 4.16 (m, 1H, H_8), 2,30 (m, 1H, H_{10}) 1.77(Cp*dia)-1.73 (s, 15H, HCp*), 0.97 (d, 2H, *J* = 7.2 Hz, H11/12), 0.89 (d, 2H, *J* = 6.6 Hz, $H_{11/12}$). **^{13}C {^{1}H} NMR** (75 MHz, $CDCl_3$) δ (ppm): 179.15(C_1), 164.47(C_7), 135.50(CH^{Ar}), 132.46(CH^{Ar}), 130.09(C_6), 126.15(CH^{Ar}), 121.62(CH^{Ar}), 87.37(C^{Cp^*}), 71.09(C_9), 68.19(C_8), 28.98(C_{10}), 19.72($C_{11/12}$), 15.40($C_{11/12}$), 9.24($CH_3^{Cp^*}$). **HRMS** (ESI+): *m/z* calculated for $C_{22}H_{29}IrNO$: 516.18729; found: 516.18730 $[M\text{-}Cl]^+$.

Ir8: Chlorido(η^5-pentamethylcyclopentadienyl)((*S*)-4-isopropyl-2-(phenyl-κC^2)-4,5-dihydrooxazole-κN)Iridium (III)
Obtained following procedure C as a yellow solid, purified using Cy/EtOAc (8:2) to yield 80%

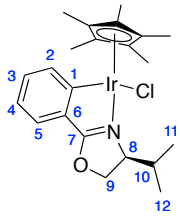

(2 diastereomers 1:0.1)
^{1}H NMR (300 MHz, $CDCl_3$) δ (ppm): 7.66 (d, 1H, J = 7.6 Hz, H_5), 7.30 (d, 1H, J = 7.5 Hz, H_2), 7.14 (t, 1H, J = 7.5 Hz, H_3), 6.90 (t, 1H, J = 7.4 Hz, H_4), 4.60 (m, 2H, H_9), 4.09 (m, 1H, H_8), 2.23 (m, 1H, H_{10}), 1,66 (s, 15H, H^{Cp^*}), 0.9 (d, 3H, J = 7.2 Hz, $H_{11/12}$), 0.83 (d, 3H, J = 6.6 Hz, $H_{11/12}$). **^{13}C {^{1}H} NMR** (101 MHz, CD_2Cl_2) δ (ppm): 178.90(C_1), 164.86(C_7), 135.73(CH^{Ar}), 131.97(CH^{Ar}), 130.49(C_6), 125.79(CH^{Ar}), 121.31(CH^{Ar}), 87.45(C^{Cp^*}), 71.26(C_9), 68.11(C_8), 28.91(C_{10}), 19.32($C_{11/12}$), 15.12($C_{11/12}$), 8.93($CH_3^{Cp^*}$). **HRMS** (ESI+): *m/z* calculated for $C_{22}H_{29}IrNO$: 516.1874; found: 516.1925 $[M\text{-}Cl]^+$.

Ir9: Chlorido(η^5-pentamethylcyclopentadienyl)((*R*)-2-(phenyl-κC^2)-4-phenyl-4,5-dihydrooxazole-κN)Iridium (III)
Obtained following procedure C as an orange solid, purified using Cy/EtOAc (9:1) to yield 87%

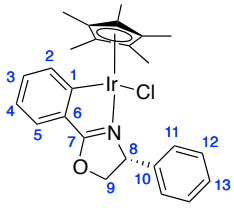

(2 diastereomers 1:1)
^{1}H NMR (300 MHz, CD_2Cl_2) δ (ppm): 7.85 (d, 1H, *J* = 7.7 Hz, H_5), 7.78 (d, 1H, *J* = 7.6 Hz, H_5), 7.72 (dd, 2H, *J* = 8.1, 1.2 Hz, H_3), 7.57 (dd, 1H, *J* = 7.6, 1.1 Hz, H_4), 7.44 – 7.30 (m, 11H^{Ar}), 7.08 (dd, 1H, *J* = 7.6, 0.9 Hz, H_2), 7.06 (dd, *J* = 7.5, 0.9 Hz, H_2), 5.45 (dd, 1H, *J* = 11.7, 9.6 Hz, H_{9a}), 5.27 (dd, 1H, *J* = 10.1, 6.1 Hz, H_{9a}), 5.19 (dd, 1H, *J* = 9.5, 8.7 Hz, H_{9b}), 5.06 (dd, 1H, *J* = 9.9, 8.5 Hz, H_{9b}), 4.59 (dd, 1H, *J* = 8.5, 6.1 Hz, H_8), 4.36 (dd, 1H, *J* = 11.8, 8.6 Hz, H_8), 1.54 (s, 15H, H^{Cp^*}), 1.49 (s, 15H, H^{Cp^*}). **^{13}C {^{1}H} NMR** (75 MHz, $CDCl_3$) δ (ppm): 182.10-181.14 (C_1), 164.02-163.29(C_7), 141.18-137.92(C_6), 135.54-135.18, 133.07-132.22, 131.21-130.55, 129.77-129.18, 129.03-128.56(4C, C_{11}), 128.72-128.18, 128.43-127.68(4C, C_{12}), 126.93-126.65, 121.84-121.77, 88.17-87.60(C^{Cp^*}), 80.08-78.04(C_8), 69.03-68.24(C_9), 9.38-9.23($CH_3^{Cp^*}$). **HRMS** (ESI+): *m/z* calculated for $C_{25}H_{27}IrNO$: 550.1716; found: 550.1721 $[M\text{-}Cl]^+$.

Ir10: Chlorido(η^5-pentamethylcyclopentadienyl)((*S*)-2-(phenyl-κC^2)-4-phenyl-4,5-dihydrooxazole-κN)Iridium (III)
Obtained following procedure C as an orange solid, purified using Cy/EtOAc (9:1) to yield 87%

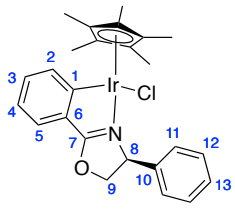

(2 diastereomers 1:1)
^{1}H NMR (300 MHz, $CDCl_3$) δ (ppm): 7.84 (d, 1H, *J* = 7.7 Hz, H_5), 7.79 (d, 1H, *J* = 7.6 Hz, H_5), 7.74 (dd, 2H, *J* = 8.1, 1.2 Hz, H_3), 7.57 (dd, 1H, *J* = 7.6, 1.1 Hz, H_4), 7.49 (dd, 1H, *J* = 7.6, 1.2 Hz, H_4), 7.47 – 7.25 (m, 10H^{Ar}), 7.08 (dd, 1H, *J* = 7.6, 0.9 Hz, H_2), 7.03 (dd, *J* = 7.5, 0.9 Hz, H_2), 5.42 (dd, 1H, *J* = 11.7, 9.6 Hz, H_{9a}), 5.29 (dd, 1H, *J* = 10.1, 6.1 Hz, H_{9a}), 5.14 (dd, 1H, *J* = 9.5, 8.7 Hz, H_{9b}), 5.05 (dd, 1H, *J* = 9.9, 8.5 Hz, H_{9b}), 4.56 (dd, 1H, *J* = 8.5, 6.1 Hz, H_8), 4.33 (dd, 1H, *J* = 11.8, 8.6 Hz, H_8), 1.54 (s, 15H, H^{Cp^*}), 1.49 (s, 15H, H^{Cp^*}). **^{13}C {^{1}H} NMR** (75 MHz, $CDCl_3$) δ (ppm): 182.10(C_1), 164.01-163.28(C_7), 141.18-137.91(C_6), 135.54-135.18, 133.07-132.23, 131.21-130.55, 129.77-129.18*, 129.03-128.56(4C, C_{11}), 128.72-128.18, 128.43-127.68(4C, C_{12}), 126.93-126.65, 121.84-121.78, 88.17-87.60(C^{Cp^*}), 80.08-78.04(C_8), 69.04-68.24(C_9), 9.38-9.22($CH_3^{Cp^*}$).
HRMS (ESI+): *m/z* calculated for $C_{25}H_{27}IrNO$: 550.17164; found: 550.17159 $[M\text{-}Cl]^+$.

X-ray crystallography analysis. A single crystal of the compound was selected, mounted onto a cryoloop, and transferred in a cold nitrogen gas stream (Oxfrod Cryostream 700). Intensity data were collected with a BRUKER Kappa-APEXII diffractometer with Mo-Kα radiation at 200K. APEX 2 suite and SAINT program (BRUKER) were used to carry out data collection, unit-cell parameters refinement, integration and data reduction. SADABS (BRUKER) was used for scaling and multi-scan absorption corrections. In the Olex2 suite[5], the structure was solved with Sir92[6] program and refined by full-matrix least-squares methods using SHELXL-14[7]. All non-hydrogen atoms were refined anisotropically. Hydrogen atoms were placed at calculated positions and refined with a riding model. CCDC 1995094 contains the supplementary crystallographic data for this paper. The data can be obtained free of charge from The Cambridge Crystallographic Data Centre via www.ccdc.cam.ac.uk/structures.

Cell culture conditions and biological assays

HeLa cell line was obtained from the American Type Culture Collection. Cells were cultivated in DMEM Glutamax High Glucose supplemented with antibiotics (penicillin, streptomycin) and 10 % fetal bovine serum, later denominated as complete medium. All culture reagents were purchased from Invitrogen.

MTT Viability Assay. The cell proliferation assay was carried out using Promega CellTiter 96® Non-Radioactive Cell Proliferation Assay according to the supplier's protocol. Briefly, 4000 cells were seeded in 96-well plates and cultivated in the presence of **Ir1-10** for 96 hours. 15 µL of MTT Dye Solution was added to each well and the plates were incubated at 37°C in a humidified 5 % CO_2 atmosphere for 4 hours. 100 µL of Stop Solution were then added to each well and absorbance was read at 570nm using Infinite F200 PRO Tecan plate reader, once formazan crystals completely solubilized. Compound concentrations that produces 50% growth inhibition (IC_{50}) were calculated from non-linear regressions of the triplicate data using Graphpad Prism software. The experiment was reproduced three times to calculate a mean value and standard deviation of these inhibiting concentrations.

xCELLigence proliferation assay and time-lapse microscopy. Two xCELLigence E-plates were calibrated for a baseline definition and HeLa cells were seeded at 2000 cells per well in 100 µL of complete medium. After 24 hours, **Ir2**, **Ir4**, **Ir8** and **Ir10** were administered at 20, 10, 5, 2.5 and 1.25 µM in quadruplicate and the cell index was measured over a period of 72 hours (Real Time Cell Analyzer, Agilent). The proliferation profiles for **Ir4** and the method for calculating a time-dependent IC_{50} are presented in Figure S4. In parallel, 50000 cells were seeded in 24-well plates and treated 24-48 hours later with either **Ir8** or DMSO vehicle. The cell behaviour was monitored in real time over 30 hours of treatment by differential phase contrast videomicroscopy using an Olympus IX83 inverted microscope with 20x objective. Time-lapse movies (1 frame per 15 min) were processed using Fiji.

HyPer-based assay. HeLa-HyPer is a stable cell line expressing the HyPer 2nd generation probe upon doxycycline induction[8]. Cells were cultivated in complete medium with Hygromycin B (0.1 mg/mL) and Blasticidin S (7.5 µg/mL). One day after induction, cells were harvested with 0.05% trypsin-EDTA solution, suspended in fresh medium, incubated in suspension for 30 min in standard growth conditions (37°C, 5% CO_2) for adaptation to a new environment, and analyzed by flow cytometry (Gallios, Beckman-Coulter, 405/488 nm laser). Before the analysis, the suspension was split into a set of samples supplemented with HEPES buffer. During the analysis, cells were gated for HyPer expression (Figure S6B) and within this gate the median ratio (M) of Ex488/FL525 and Ex405/FL525 signals (denoted after as Em488/405) was determined. Intracellular peroxide concentration was assessed using HyPer-index[9] which was quantified in % as follows: $H = (M_{sample}-M_{DMSO})/(M_{H2O2}-M_{DMSO})$ where M_{DMSO} and M_{H2O2} correspond to the median ratio values obtained for the negative and positive controls respectively. Two independent experiments were carried out: first, a kinetic study of the probe's state over time after direct administration of **Ir2** at 2.5-20 µM. Second, 10 µM **Ir1-10** were administered and the suspensions were analyzed after 60 min. Both experiments were compared to a 1% DMSO negative control. To induce the complete oxidation of the probe, 140-500 µM H_2O_2 were added and cells were analyzed after 5 min as positive control.

Cleaved-Caspase-3 Western Blot analysis. 10^6 HeLa cells were seeded in 60 mm culture dishes and incubated for 16 h in complete medium. For each dish, 20 µL of drug was added (1 mM stock in DMSO, 10 µM final). After quick homogenization, cells were incubated at 37°C 5% CO_2 in a humidified atmosphere for 6, 12 or 24 h. Non-treated cells, cells exposed to 1% DMSO or to 10 µM Etoposide were used as negative and positive controls respectively. Cells were harvested in cold PBS and lysed in RIPA buffer, supplemented with protease and phosphatase inhibitors. Protein titration was carried out using the microBCA assay-kit (based on Pierce BCA). Samples were analyzed by SDS-PAGE on 4-20 % gradient polyacrylamide gels (BioRad) and transferred onto 20 µm nitrocellulose membranes. Proteins were stained with Ponceau S (Figure S5). Membranes were blocked and incubated with a Rabbit-anti-Cleaved Caspase 3 (Cell Signaling #9661) antibody, a HRP-linked secondary antibody (Cell Signaling #7074) and the luminol revelation kit (BioRad).

NADH quantification. Ir1-10 (10 µM) and NADH (100 µM) were incubated for 150 min at 37°C in 1% MeOH / 99% 5 mM Phosphate Buffer pH 7.4. Mixtures were analyzed by UV-Vis spectroscopy at 20°C. The concentration of NADH was calculated using the extinction coefficient ε_{340} = 6200 $M^{-1}cm^{-1}$. Turnover number (TON) is defined as the number of moles of NADH that a mole of catalyst (**Ir1-10**) can convert within 150 min. The experiment was reproduced three times to calculate a mean and standard deviation. TON values for each complex are reported in Table S4.

Amplex Red® HRP-linked enzymatic assay. Ir1-10 (50 µL in PB, 10% mol final) or H_2O_2 standards (150 nM - 5 µM final), the Amplex substrate and HRP (25 µL, 5 µM and 1 U/mL final) and NADH containing SOD[10] (25 µL, 100 µM and 40 U/mL final) were sequentially dispensed in a black 96-well plate. Fluorescence (exc. 520nm em. 595nm) was recorded every 5 min during 150 min. This experiment was performed three times in triplicate to calculate a mean and standard deviation of the values of produced H_2O_2 (µM).

Figures S1-S8

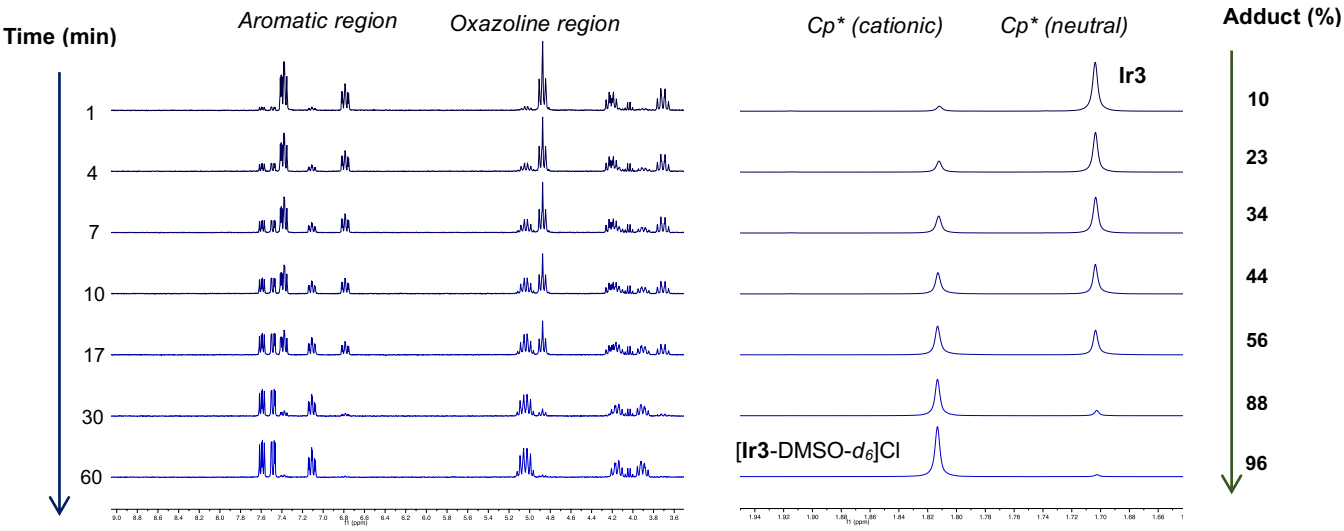

Figure S1. ^{1}H NMR study of the solvolysis of **Ir3** in DMSO-d_6. The Cp* signals were integrated to quantify the share of neutral and exchanged forms at each timepoint.

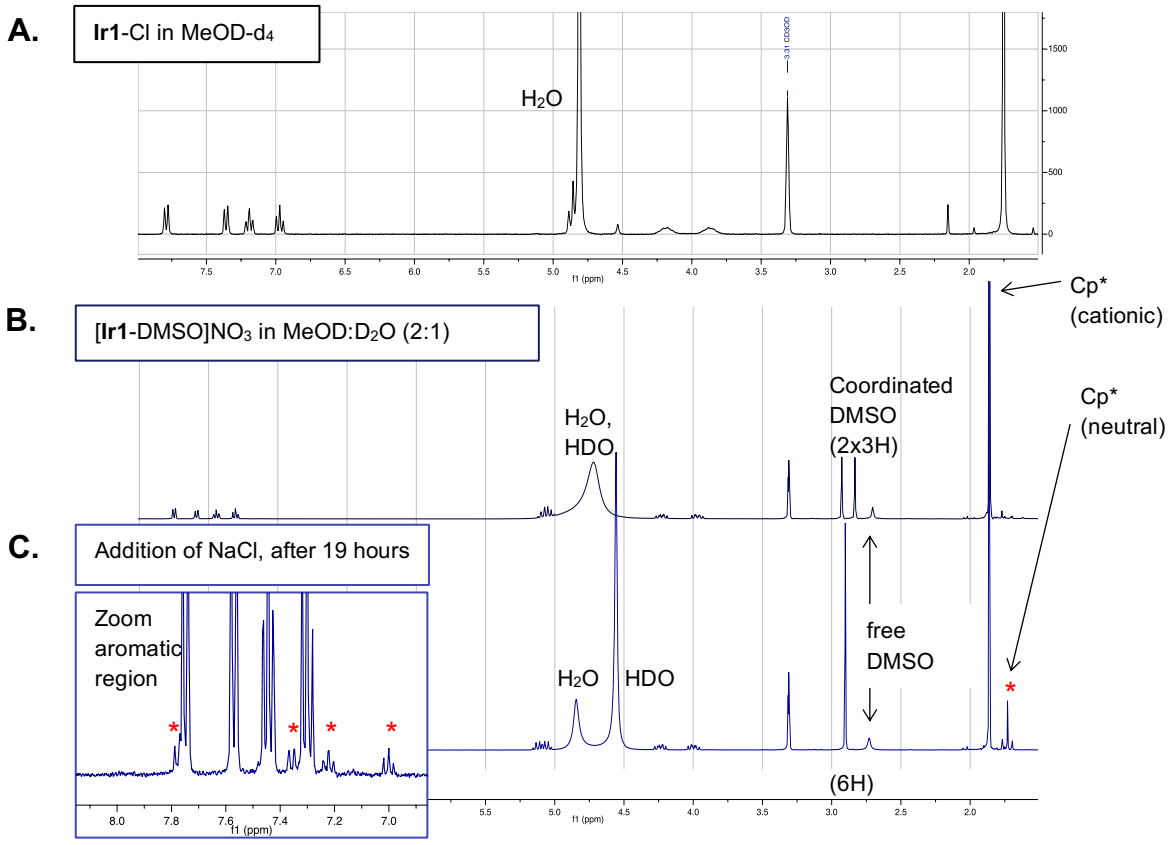

Figure S2. ^{1}H NMR study of a cationic DMSO adduct in presence of water and excess of NaCl. **A.** ^{1}H NMR spectrum of **Ir1** in MeOD. **B.** ^{1}H NMR spectrum of [**Ir1**-DMSO]NO_3 in MeOD:D_2O (2:1). [**Ir1**-DMSO]NO_3 was obtained as follows: **Ir1** was dissolved in CH_2Cl_2 with $AgNO_3$ (1.0 eq.) and DMSO (1.1 eq.) was added after 15 min. The solution was stirred at r.t. for 1 h and evaporated to dryness to afford [**Ir1**-DMSO]NO_3 as a crude product. **C.** ^{1}H NMR spectrum of [**Ir1**-DMSO]NO_3 in MeOD:D_2O (2:1) with saturating (1.1 M) NaCl. The neutral **Ir1** form (*) is detected 1 h after adding ca. 50 mg NaCl in the NMR tube containing [**Ir1**-DMSO]NO_3.

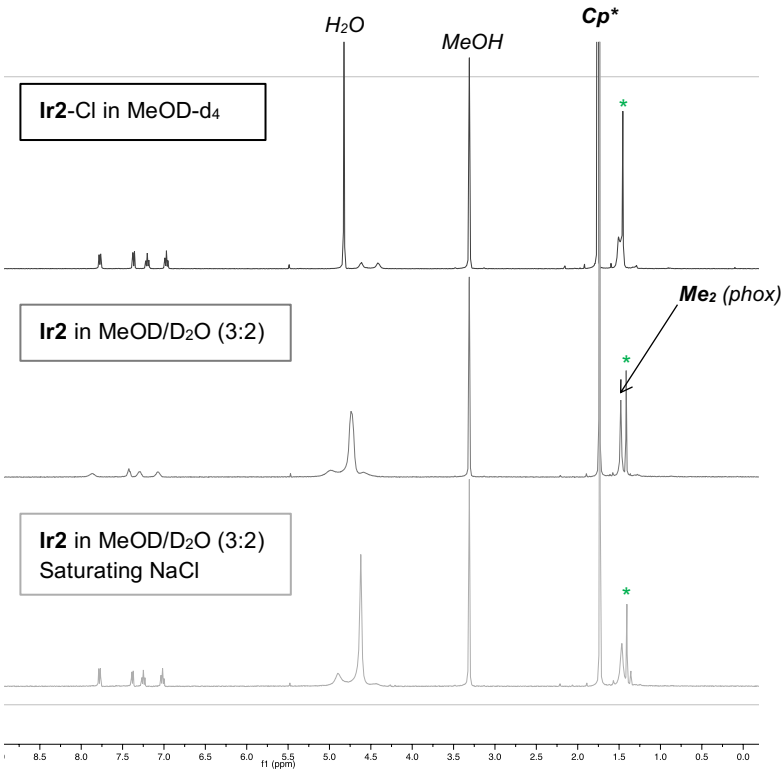

Figure S3. ^{1}H NMR spectra of **Ir2** (21 mM) in MeOD-d_4, MeOD-d_4 / D_2O (3:2) and with saturating NaCl. * residual cyclohexane

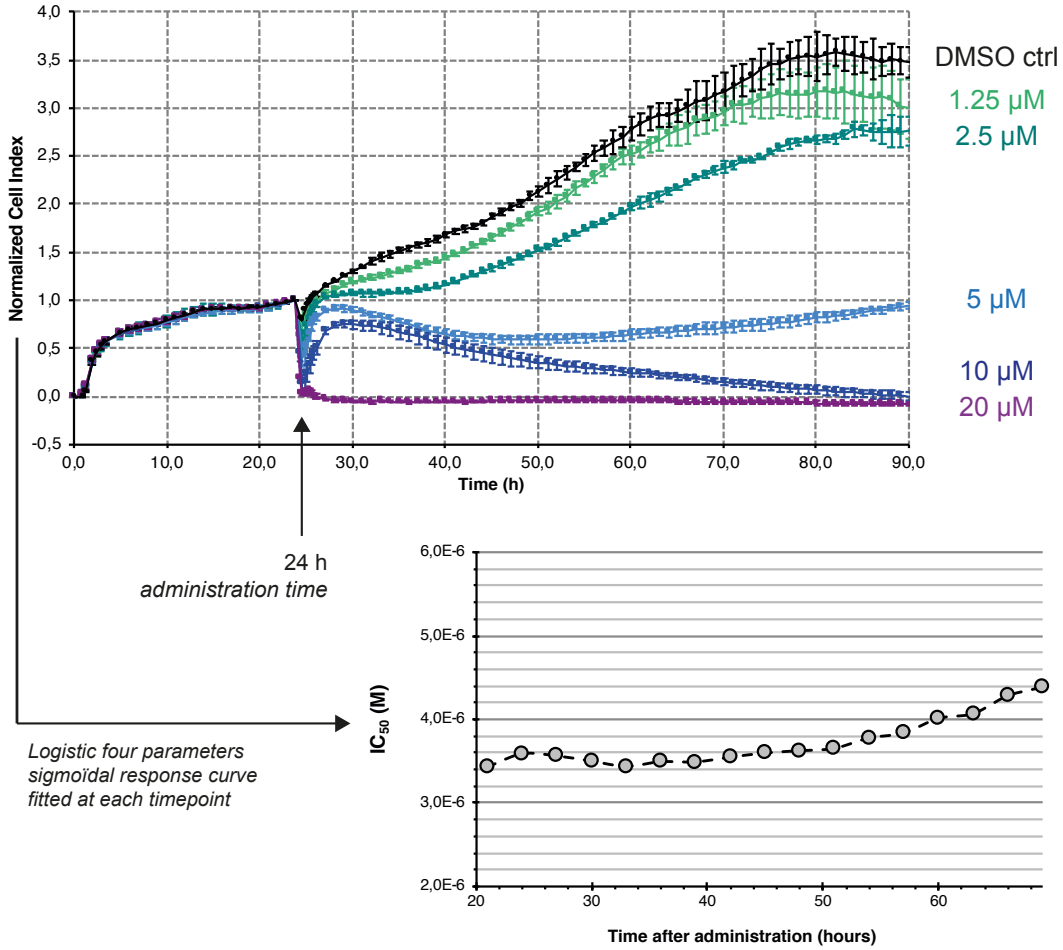

Figure S4. xCELLigence® RTCA proliferation profiles of HeLa cells cultivated in the presence of **Ir8** depending on the indicated concentration. DMSO ctrl: vehicle only. The mean Normalized Cell Index at each concentration was processed by the RTCA software to determine the time-dependent IC_{50}.

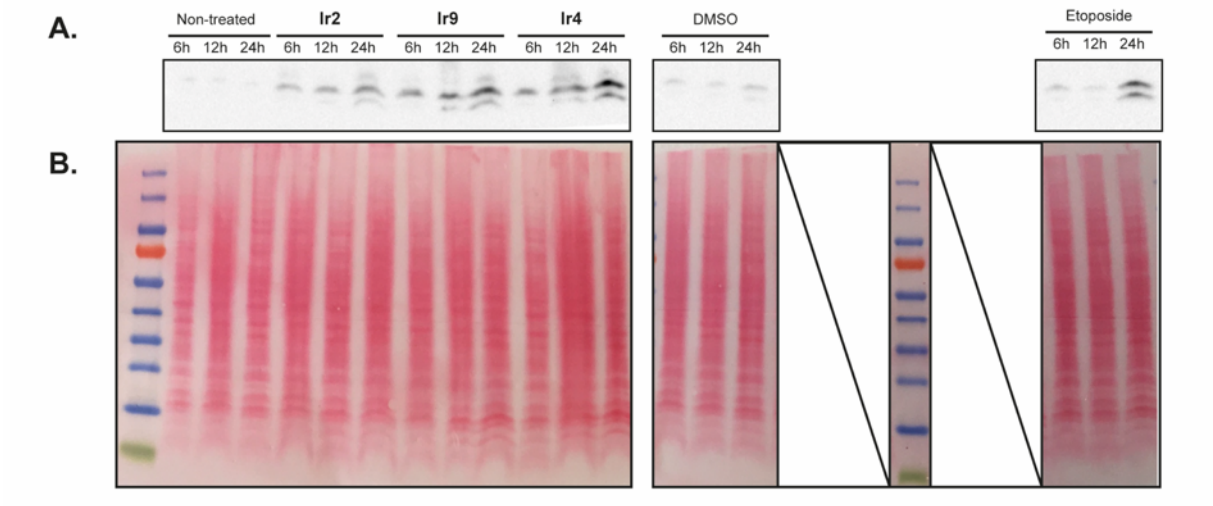

Figure S5. **A.** Detection of cleaved caspase-3 by western blotting as in Figure 3. **B.** Ponceau S staining of the immunoblot showing equal protein load.

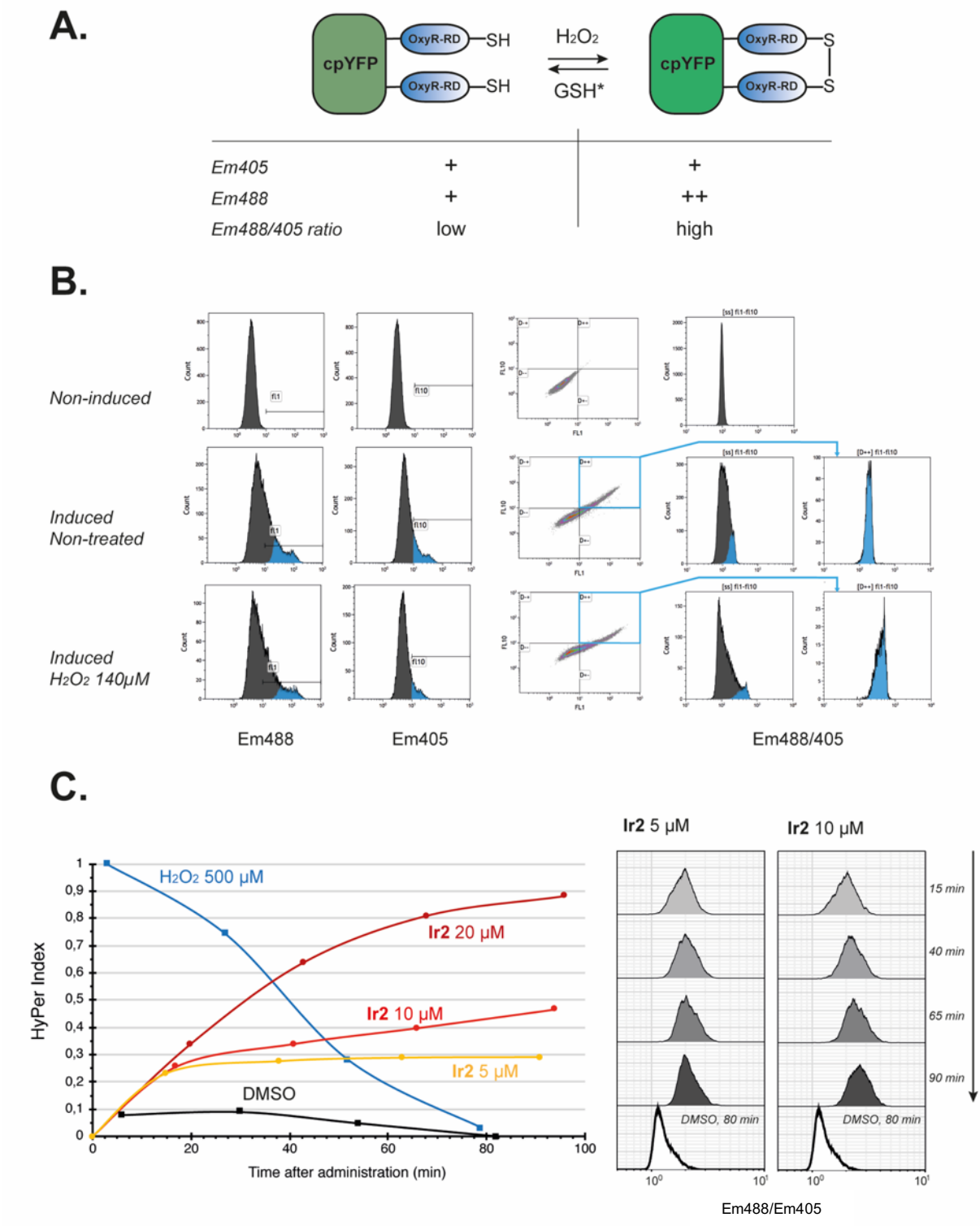

Figure S6. A. Principle of HyPer probe. Emission intensity following excitation at 405 nm and 488 nm is indicated. *Several reductases, in association with glutathione, are able to reduce the probe's disulfide bond. **B.** Gating strategy applied to assess the Em488/405 ratio. After doxycycline-induction of Hyper expression, HyPer expressing cells are gated and appear blue on histograms. **C.** Kinetics of the HyPer index and dose-dependent response to **Ir2** treatment.

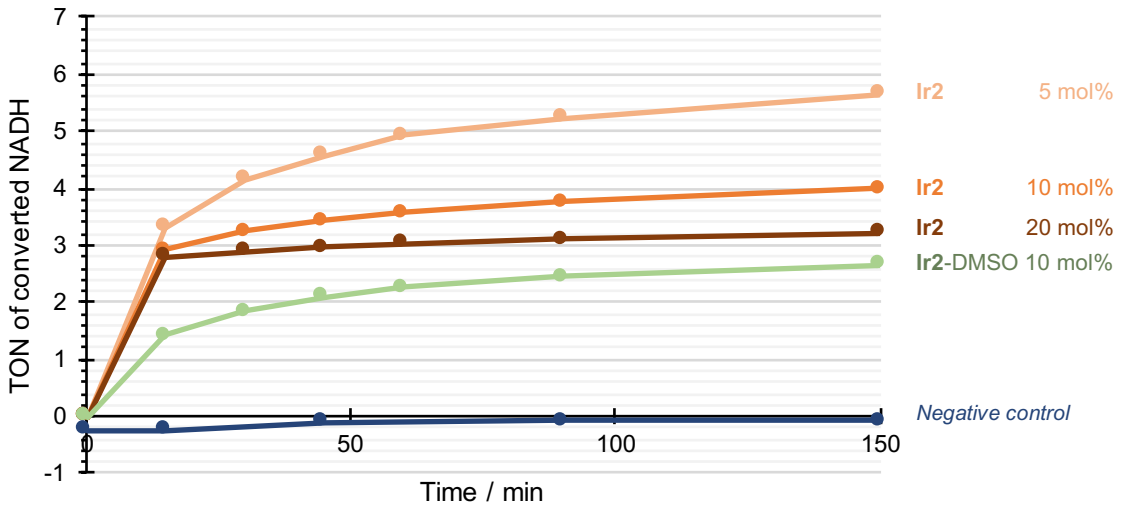

Figure S7. NADH *in vitro* quantification in presence of various concentrations of **Ir2** in PB:MeOH (99:1) evaluated by absorbance readings at 340 nm. Results are expressed in TON of converted substrate. Experiment was also performed in the presence of DMSO (1 eq): **Ir2**-DMSO. Negative control: no **Ir2.**

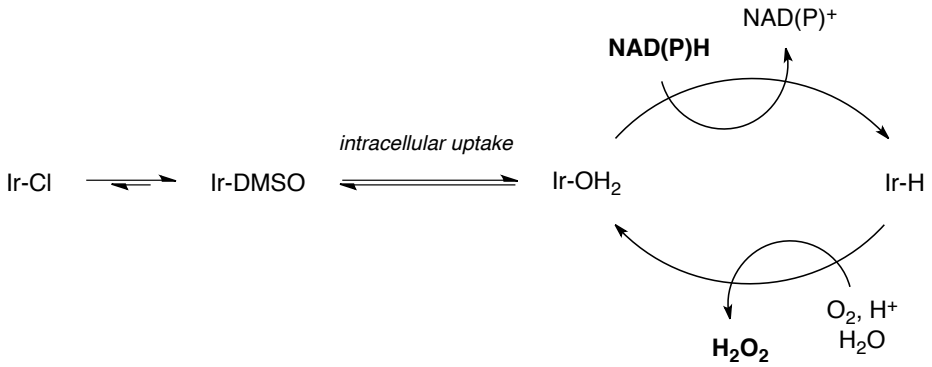

Figure S8. Possible catalytic pathway for the intracellular production of H_2O_2 by half-sandwich iridium complexes, adapted from Z. Liu, P.J. Sadler et al. (Angew. Chem. Int. Ed., 2014)[11]

Videomicroscopy

Time-lapse movies (1 frame per 15 min) of HeLa cells cultivated in the presence of 2.5 and 5 μM Ir8. Ctrl: DMSO vehicle.

2.5 μM **Ir8**: http://www.rsc.org/suppdata/d0/dt/d0dt03414b/d0dt03414b1.mov

5 μM **Ir8**: http://www.rsc.org/suppdata/d0/dt/d0dt03414b/d0dt03414b2.mov

Ctrl (DMSO vehicle): http://www.rsc.org/suppdata/d0/dt/d0dt03414b/d0dt03414b3.mov

Tables S1-S4

Table S1. Crystal data and structure refinement for **Ir1**.

Empirical formula	$C_{19}H_{23}ClIrNO$
Formula weight	509.03
Temperature/K	200(2)
Crystal system	monoclinic
Space group	Cc
a/Å	10.2639(3)
b/Å	13.4056(3)
c/Å	13.9884(4)
α/°	90
β/°	110.5530(10)
γ/°	90
Volume/Å^3	1802.20(8)
Z	4
ρ_{calc}g/cm^3	1.876
μ/mm^{-1}	7.560
F(000)	984.0
Crystal size/mm^3	0.17 × 0.15 × 0.12
Radiation	MoKα (λ = 0.71073)
2Θ range for data collection/°	5.216 to 64.338
Index ranges	-15 ≤ h ≤ 15, -19 ≤ k ≤ 20, -20 ≤ l ≤ 20
Reflections collected	18576
Independent reflections	6195 [R_{int} = 0.0161, R_{sigma} = 0.0179]
Data/restraints/parameters	6195/2/213
Goodness-of-fit on F^2	1.043
Final R indexes [I>=2σ (I)]	R_1 = 0.0149, wR_2 = 0.0337
Final R indexes [all data]	R_1 = 0.0161, wR_2 = 0.0341
Largest diff. peak/hole / e Å^{-3}	1.45/-0.55
Flack parameter	-0.022(4)
CCDC deposition number	1995094

Table S2. Selected geometrical parameters for **Ir1**

Selected bond lengths (Å)		
Ir1	Cl1	2.4085(9)
Ir1	N1	2.076(3)
Ir1	C5	2.055(3)
Ir1	C10	2.149(4)
Ir1	C11	2.156(3)
Ir1	C12	2.236(4)
Ir1	C13	2.236(3)
Ir1	C14	2.150(3)
N1	C1	1.284(5)
N1	C2	1.466(4)
O1	C1	1.342(5)
O1	C3	1.466(5)
C1	C4	1.437(6)
C2	C3	1.523(6)
C4	C5	1.415(5)
C4	C9	1.403(5)
C5	C6	1.394(5)
C6	C7	1.396(5)
C7	C8	1.369(7)
C8	C9	1.384(6)

Angles between planes		
plane 1 *(C4 > C9)*	plane 2 *(N1 O1 C1 C2 C3)*	2.0 °

Distances from plane		
C2	plane 2	0.106 Å
C3	Plane 2	-0.08 Å

Table S3. Half-lives (min) of **Ir1-10** in DMSO-d_6

	Ir1	**Ir2**	**Ir3**	**Ir4**	**Ir5**	**Ir6**	**Ir7**	**Ir8**	**Ir9**	**Ir10**
Half-lives (min)	2	6	12	5	270	9	180	180	5	5

Table S4. TON (2.5 h) of converted NADH upon catalysis by **Ir1-10** (10 mol%) at 37°C

	Ir1	**Ir2**	**Ir3**	**Ir4**	**Ir5**	**Ir6**	**Ir7**	**Ir8**	**Ir9**	**Ir10**
TON	2.34 ± 0.61	3.68 ± 0.65	3.26 ± 0.57	2.67 ± 0.66	1.46 ± 0.20	1.29 ± 0.11	2.43 ± 0.27	2.21 ± 0.27	2.87 ± 0.25	2.74 ± 0.05

References

1 S. DakoviC, L. LiHEiC-Turni, S. I. Kirin, V. VinkoviC, Z. Raza, A. Suste and V. SunjiC, Enantioselectivity in cyclopropanation catalyzed by Cu(I) complexes increased by TTstacking of two monodentate oxazoline ligands, *J. Mol. Cat.*, 1997, **118**, 27–31.

2 J. H. Barnard, C. Wang, N. G. Berry and J. Xiao, Long-range metal–ligand bifunctional catalysis: cyclometallated iridium catalysts for the mild and rapid dehydrogenation of formic acid, *Chem. Sci.*, 2013, **4**, 1234.

3 D. L. Davies, O. Al-Duaij, J. Fawcett, M. Giardiello, S. T. Hilton and D. R. Russell, Room-temperature cyclometallation of amines, imines and oxazolines with [MCl 2 Cp*] 2 (M = Rh, Ir) and [RuCl 2 (p-cymene)] 2, *Dalton Trans.*, 2003, 4132–4138.

4 Y. Boutadla, D. L. Davies, R. C. Jones and K. Singh, The Scope of Ambiphilic Acetate-Assisted Cyclometallation with Half-Sandwich Complexes of Iridium, Rhodium and Ruthenium, *Chemistry - A European Journal*, 2011, **17**, 3438–3448.

5 O. V. Dolomanov, L. J. Bourhis, R. J. Gildea, J. A. K. Howard and H. Puschmann, *OLEX2* : a complete structure solution, refinement and analysis program, *J Appl Crystallogr*, 2009, **42**, 339–341.

6 A. Altomare, G. Cascarano, C. Giacovazzo, A. Guagliardi, M. C. Burla, G. Polidori and M. Camalli, *SIR* 92 – a program for automatic solution of crystal structures by direct methods, *J Appl Crystallogr*, 1994, **27**, 435–435.

7 G. M. Sheldrick, Crystal structure refinement with *SHELXL*, *Acta Crystallogr C Struct Chem*, 2015, **71**, 3–8.

8 C. Gauron, F. Meda, E. Dupont, S. Albadri, N. Quenech'Du, E. Ipendey, M. Volovitch, F. Del Bene, A. Joliot, C. Rampon and S. Vriz, Hydrogen peroxide (H 2 O 2) controls axon pathfinding during zebrafish development, *Developmental Biology*, 2016, **414**, 133–141.

9 O. G. Lyublinskaya, Ju. S. Ivanova, N. A. Pugovkina, I. V. Kozhukharova, Z. V. Kovaleva, A. N. Shatrova, N. D. Aksenov, V. V. Zenin, Yu. A. Kaulin, I. A. Gamaley and N. N. Nikolsky, Redox environment in stem and differentiated cells: A quantitative approach, *Redox Biology*, 2017, **12**, 758–769.

10 T. V. Votyakova and I. J. Reynolds, Detection of hydrogen peroxide with Amplex Red: interference by NADH and reduced glutathione auto-oxidation, *Archives of Biochemistry and Biophysics*, 2004, **431**, 138–144.

11 Z. Liu, I. Romero-Canelón, B. Qamar, J. M. Hearn, A. Habtemariam, N. P. E. Barry, A. M. Pizarro, G. J. Clarkson and P. J. Sadler, The Potent Oxidant Anticancer Activity of Organoiridium Catalysts, *Angewandte Chemie International Edition*, 2014, **53**, 3941–3946.

Author Contributions

R.R.: Lead chemical and biological data acquisition, writing of original draft; J.Z.: Project initiation; S.T.: Contribution to manuscript editing; L-M. C.: Structural data acquisition; A.M.: Supporting flow cytometry data acquisition and analysis; C.B.: Formal analysis of chemical data, contribution to manuscript editing; A.K.: Formal analysis of biological data; contribution to manuscript editing; M.S. and J. S-T.: Data curation, project administration and data validation, equal contribution to manuscript editing

Annexes: NMR spectra

L5

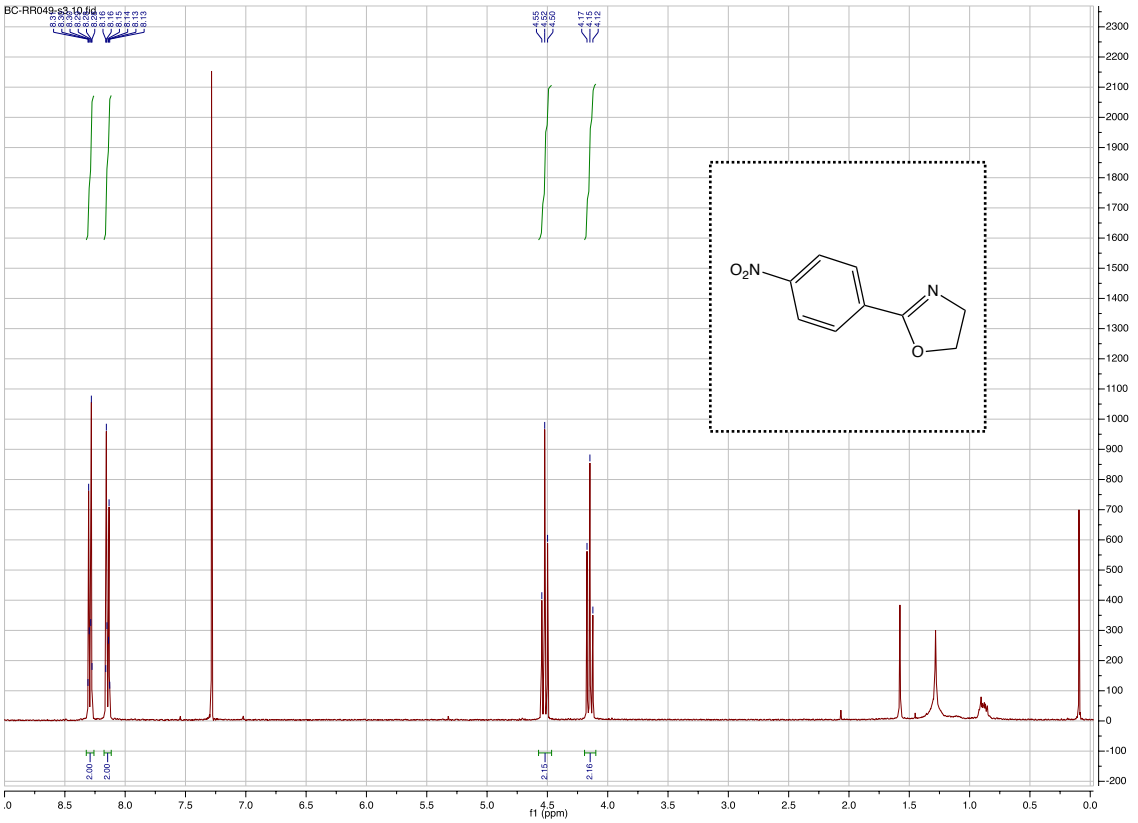

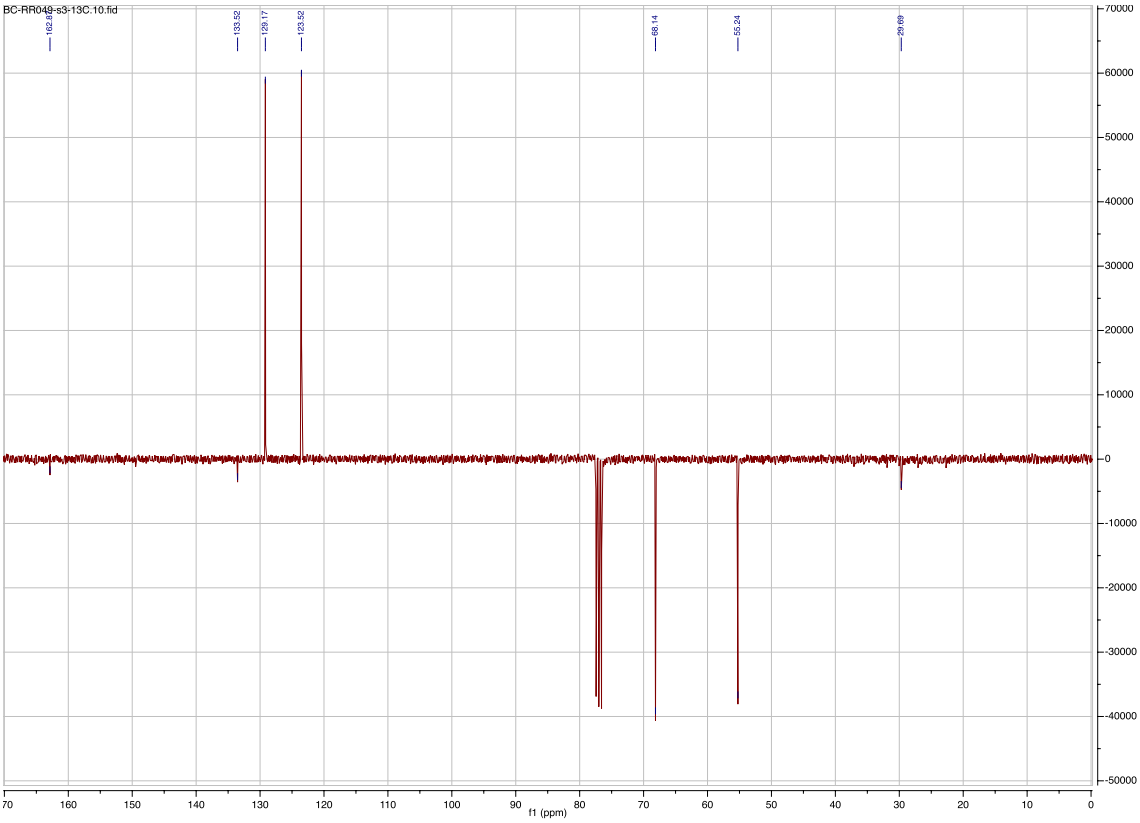

L7

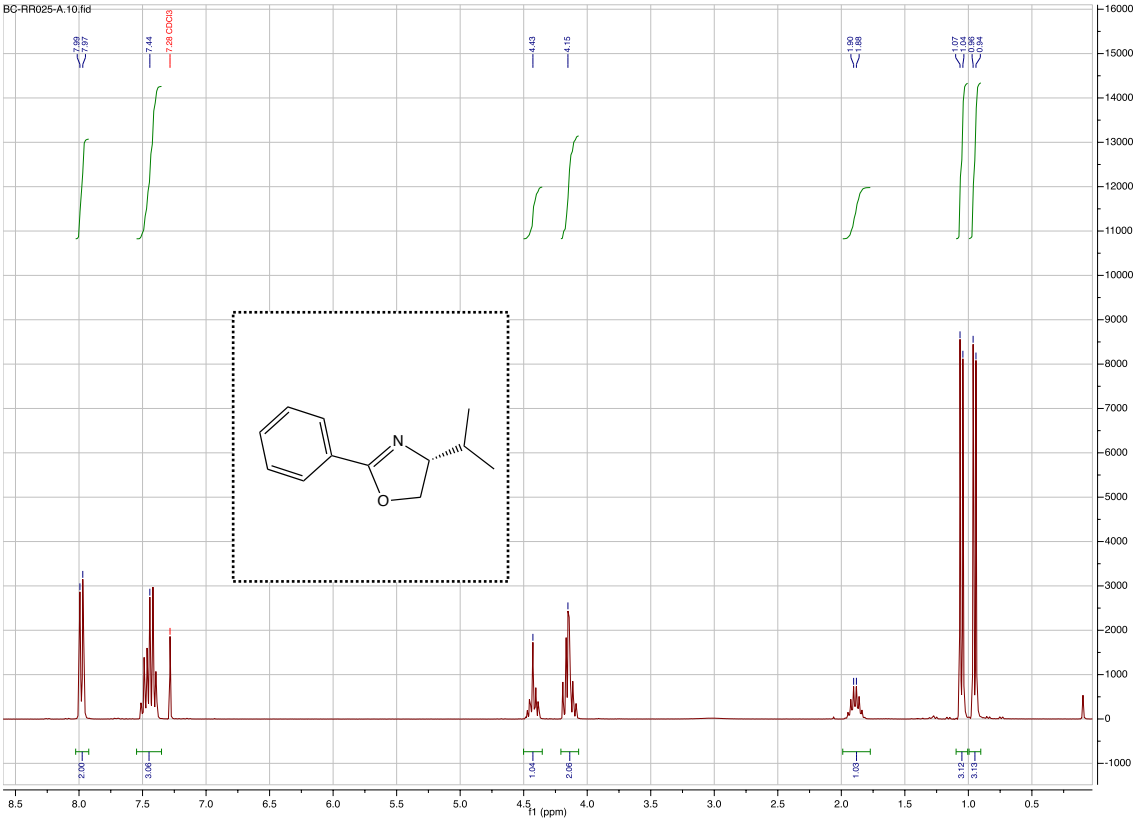
BC-RR025-A.10.fid
7.99
7.97
7.44
7.28 CDCl3
4.43
4.15
1.90
1.88
1.07
1.04
0.98
0.94
2.00
3.08
1.04
2.08
1.03
3.12
3.13
f1 (ppm)

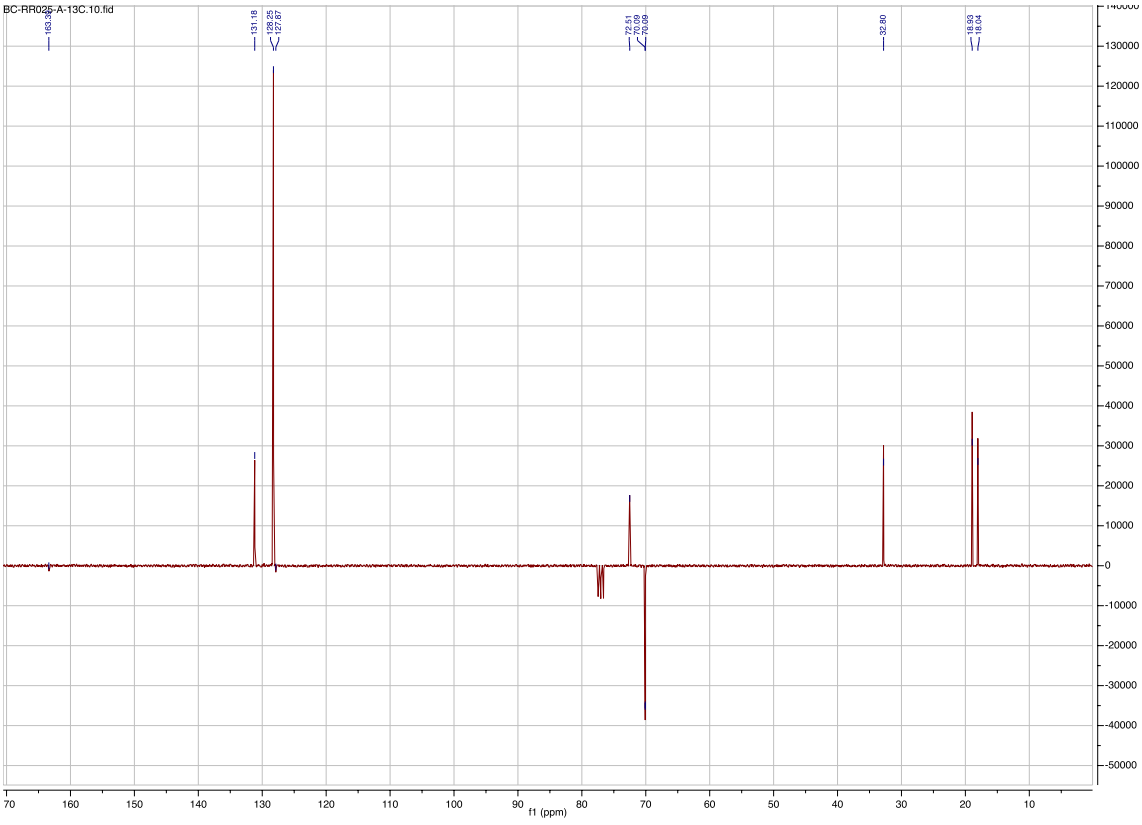
BC-RR025-A-13C.10.fid
163.36
131.18
128.25
127.87
72.51
70.09
70.04
32.80
18.89
18.04
f1 (ppm)

Ir3

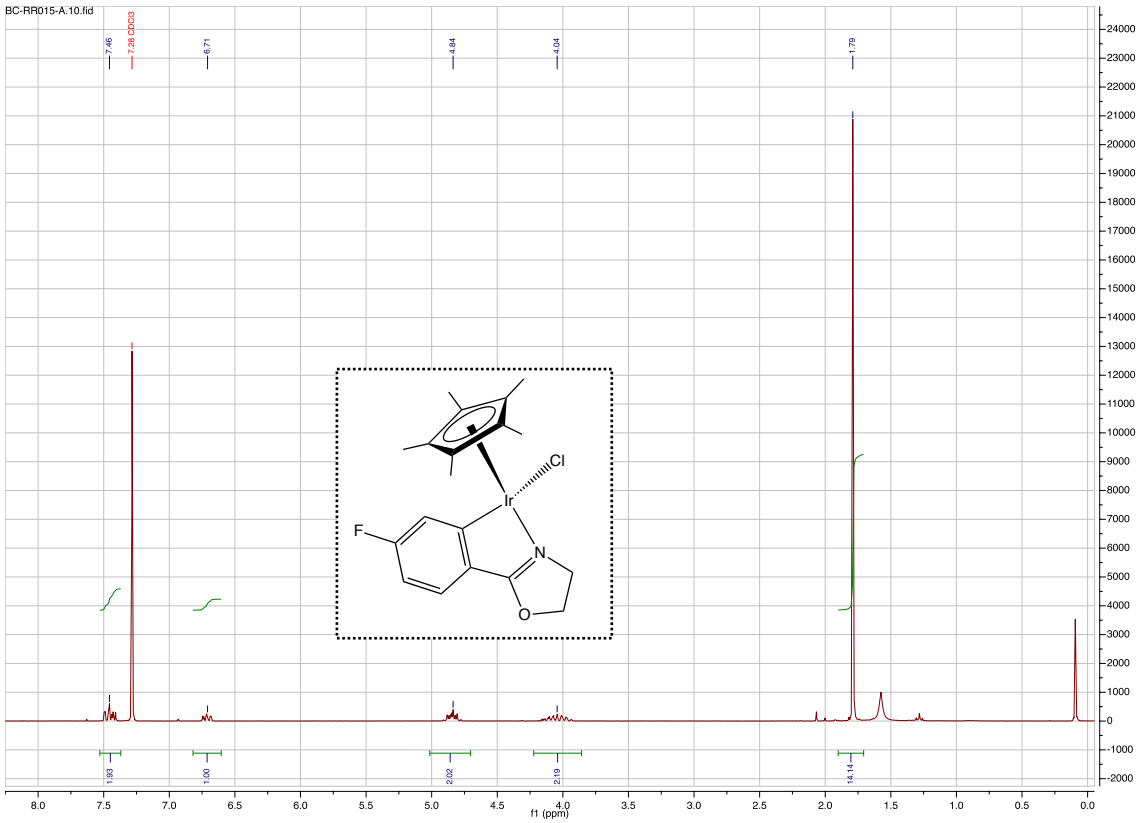
BC-RR015-A.10.fid
7.46
7.28 CDCl3
6.71
4.84
4.04
1.79
Cl
Ir
F
N
O
1.93
1.00
2.02
2.19
14.14
f1 (ppm)

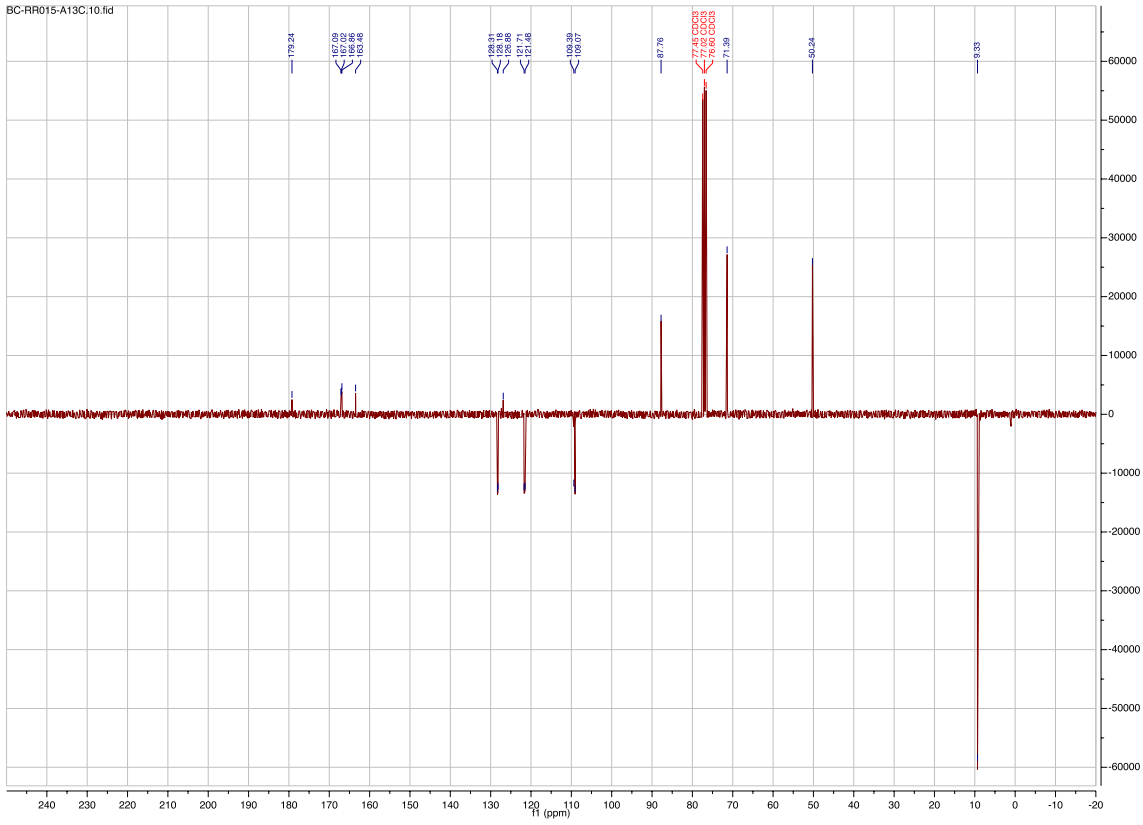
BC-RR015-A13C.10.fid
179.24
167.09
167.02
165.86
163.46
128.31
128.18
125.86
121.71
121.48
109.39
109.07
87.76
77.48 CDCl3
77.16 CDCl3
76.80 CDCl3
71.39
50.24
9.33
f1 (ppm)

Ir4

BC-BG022-PF.10.fid

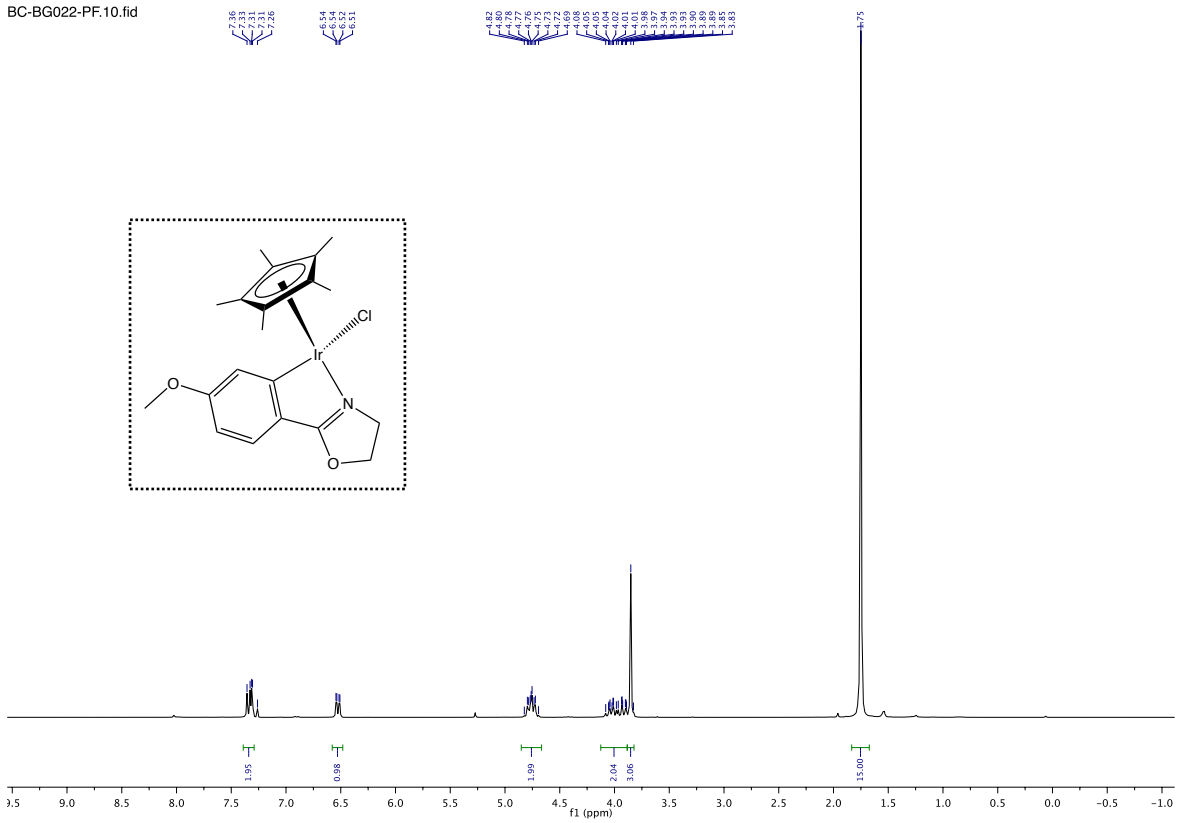

BC-BG022-PF.11.fid

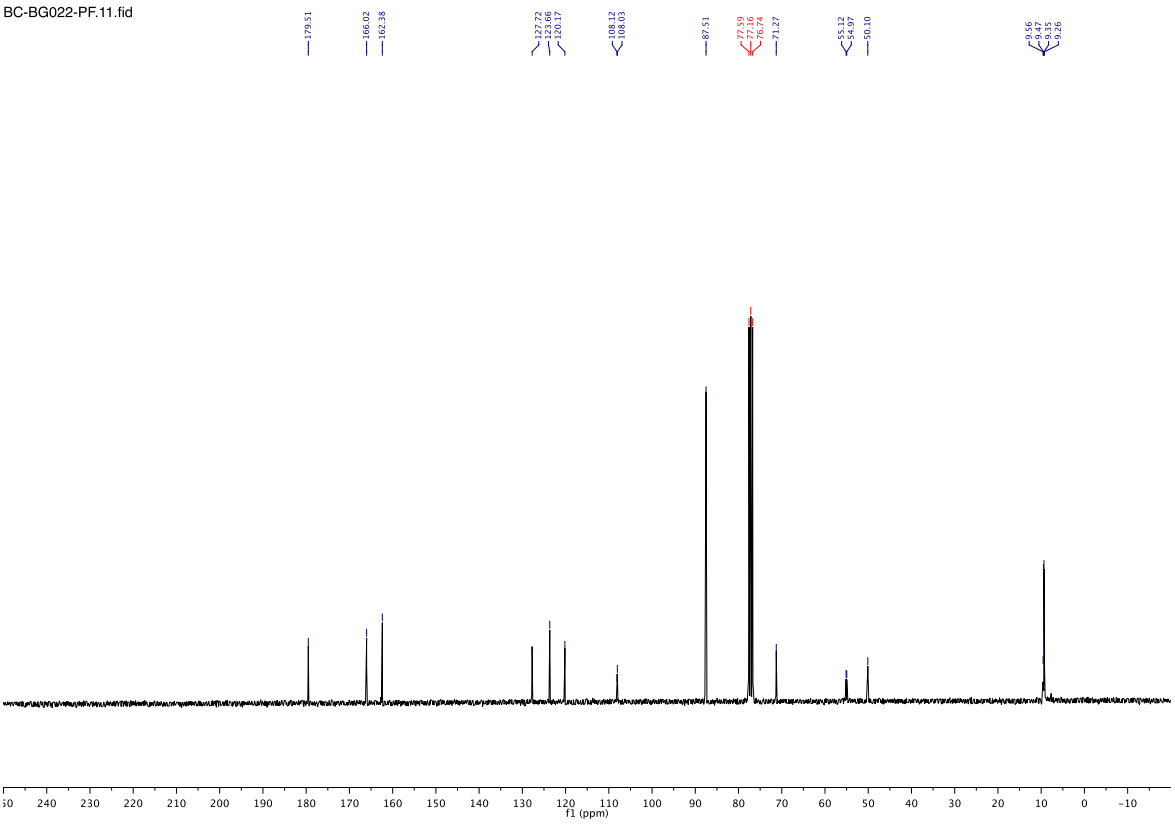

Ir5

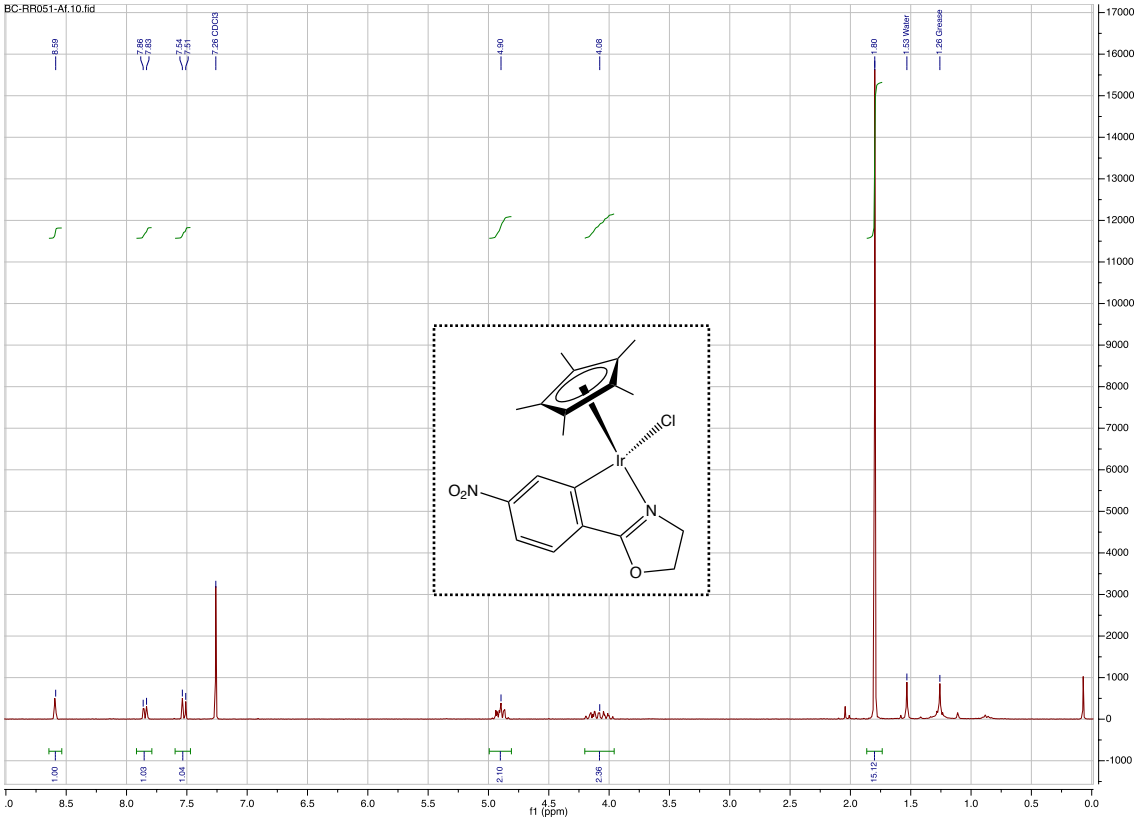
BC-RR051-Af.10.fid
8.59
7.86
7.83
7.54
7.51
7.26 CDCl3
4.90
4.08
1.80
1.53 Water
1.26 Grease
Cl
Ir
O2N
N
O
1.00
1.03
1.04
2.10
2.36
15.12
f1 (ppm)

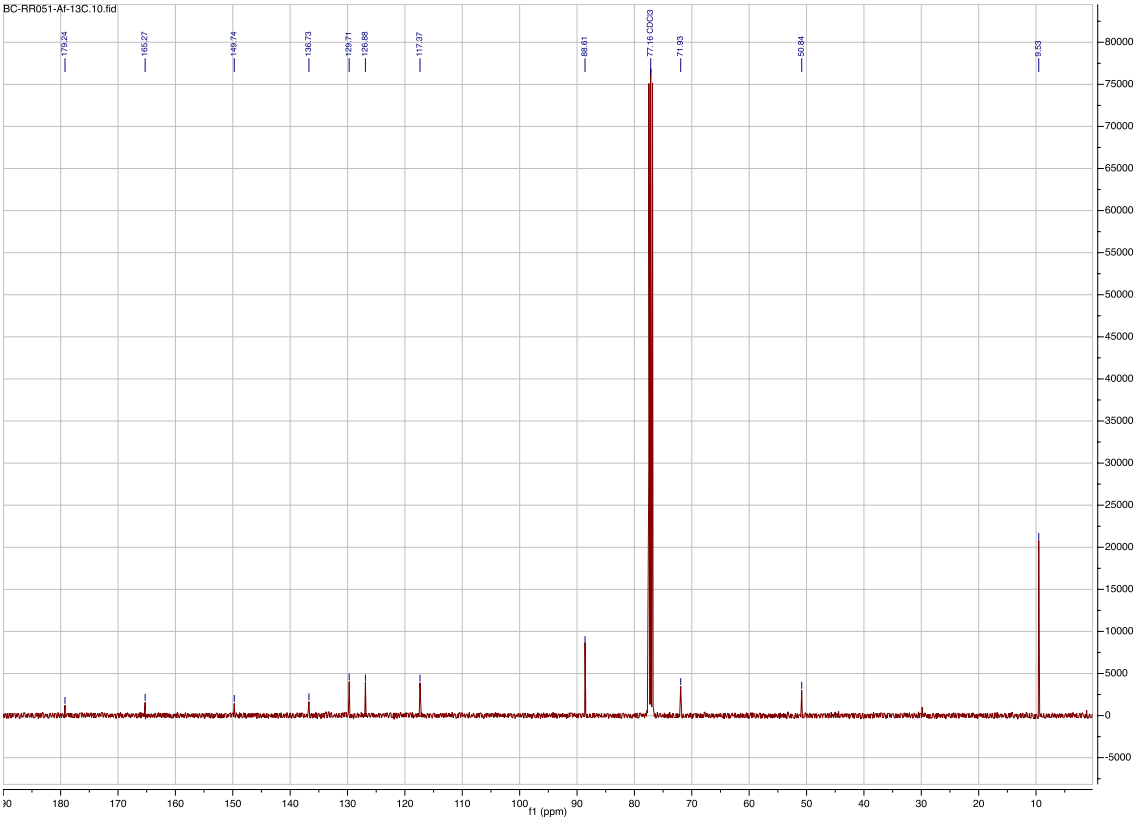
BC-RR051-Af-13C.10.fid
179.24
165.27
149.74
136.73
129.71
125.88
117.37
88.61
77.16 CDCl3
71.83
50.84
9.53
f1 (ppm)

Ir6

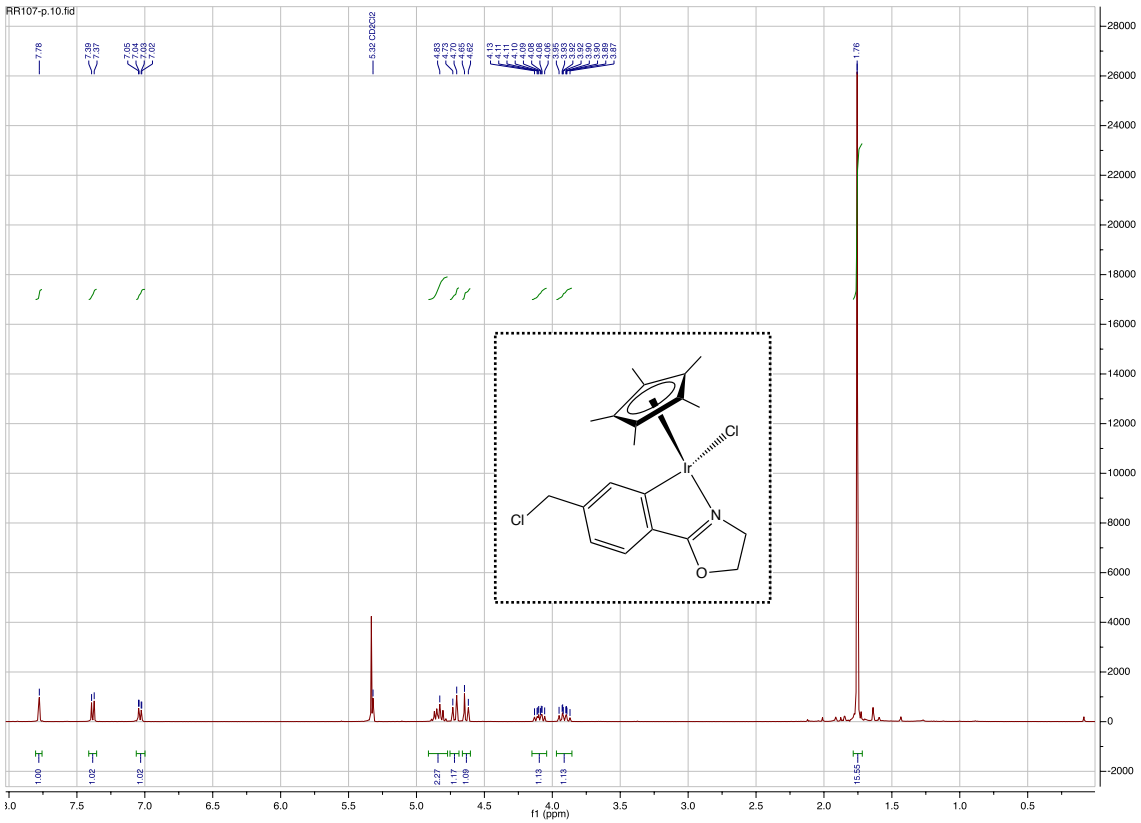
RR107-p.10.fid
7.78
7.39
7.37
7.05
7.04
7.03
7.02
5.32 CD2Cl2
4.83
4.73
4.70
4.65
4.62
4.13
4.11
4.11
4.10
4.09
4.08
4.07
4.06
3.95
3.93
3.92
3.92
3.90
3.90
3.89
3.88
3.87
1.76
Cl
Ir
Cl
N
O
1.00
1.02
1.02
2.27
1.17
1.09
1.13
1.13
15.55
f1 (ppm)

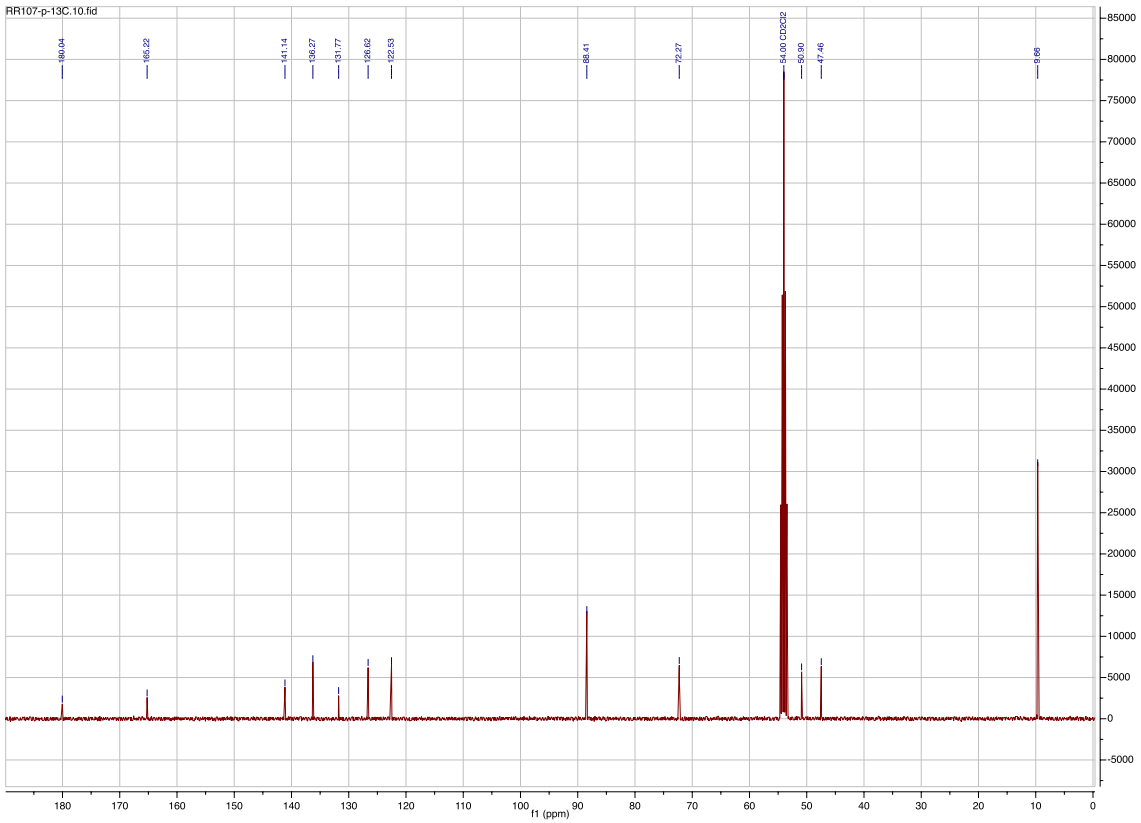
RR107-p-13C.10.fid
180.04
165.22
141.14
136.27
131.77
126.62
122.53
88.41
72.27
54.00 CD2Cl2
50.90
47.46
9.66
f1 (ppm)

Ir7

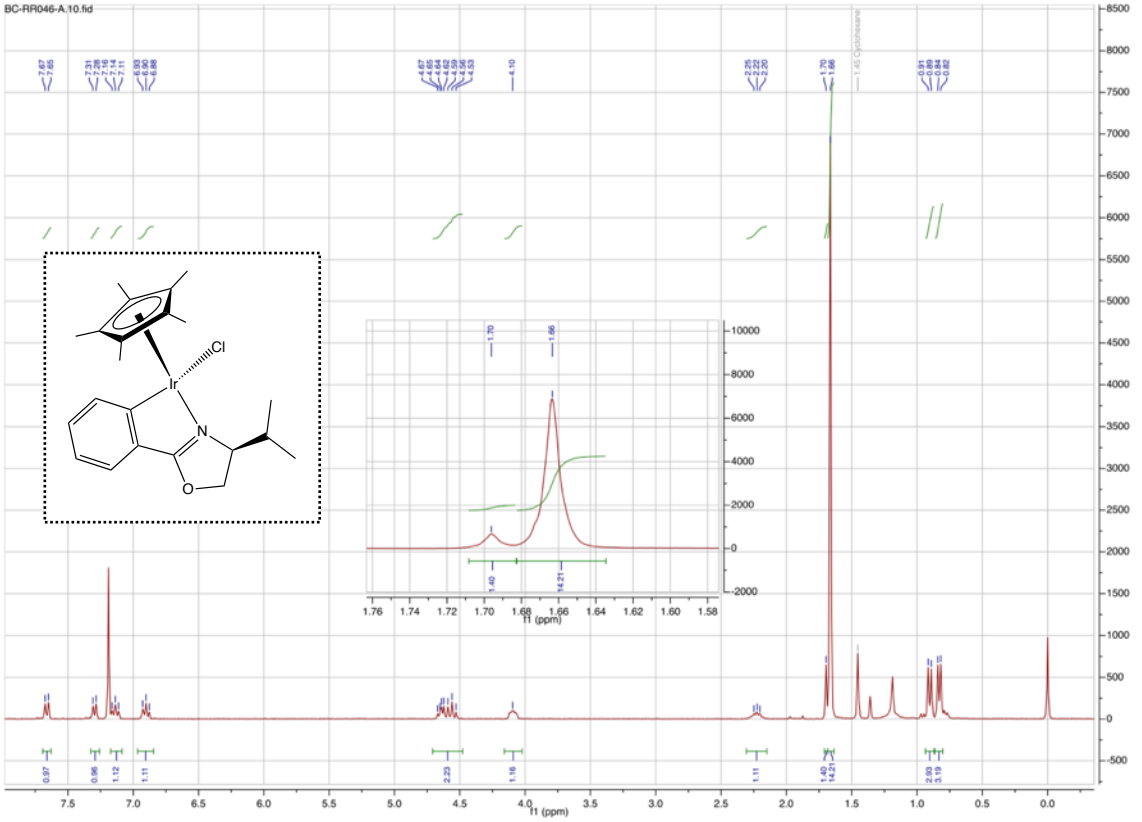

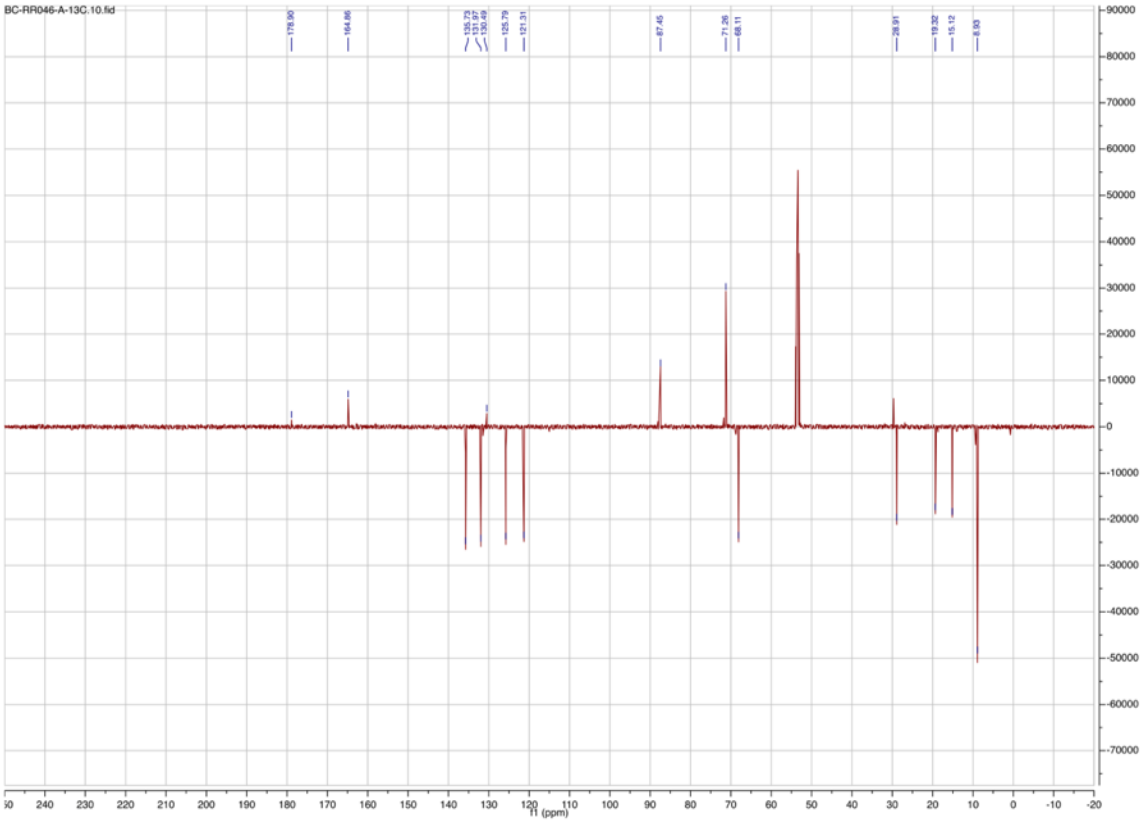

Ir8

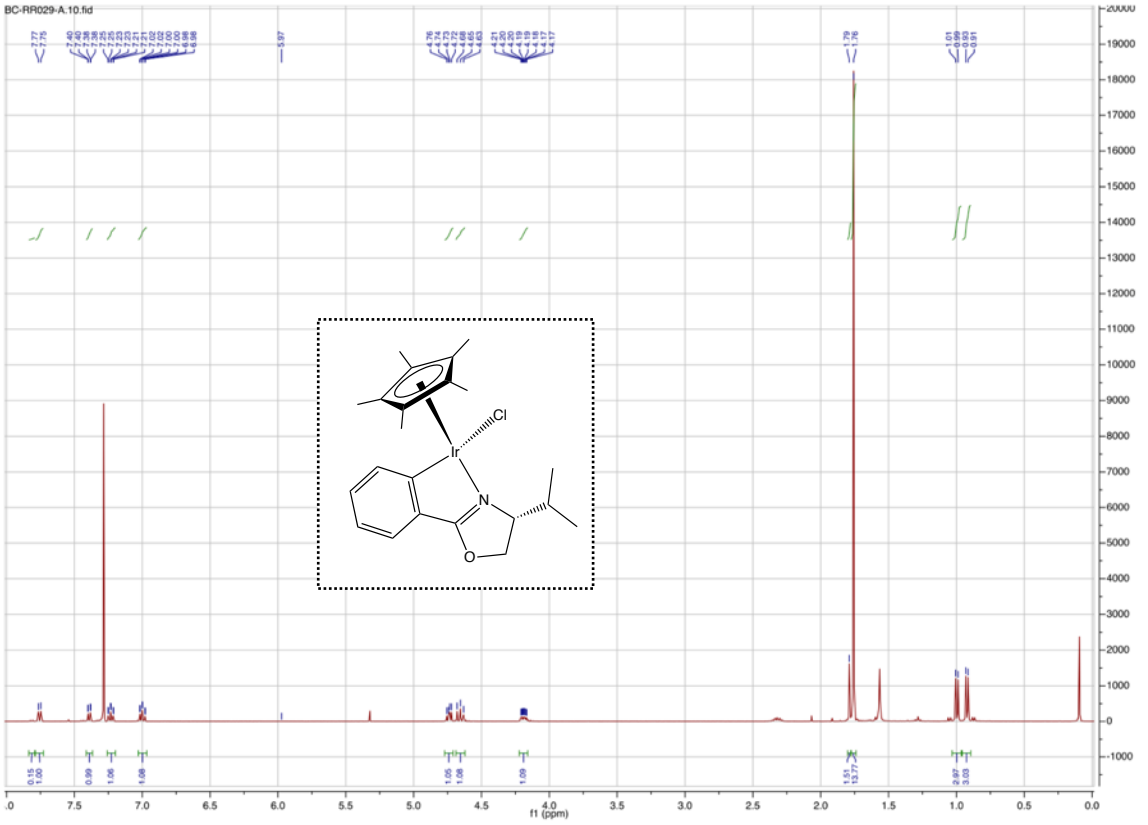

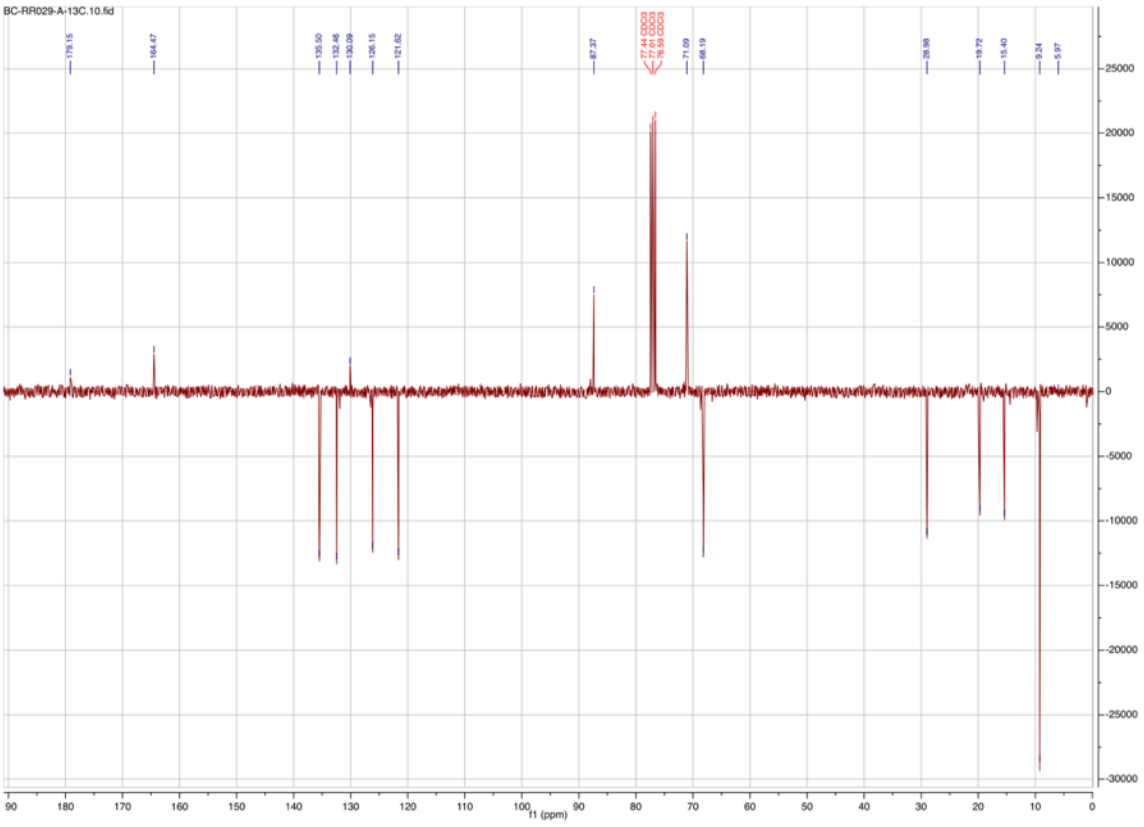

Ir9

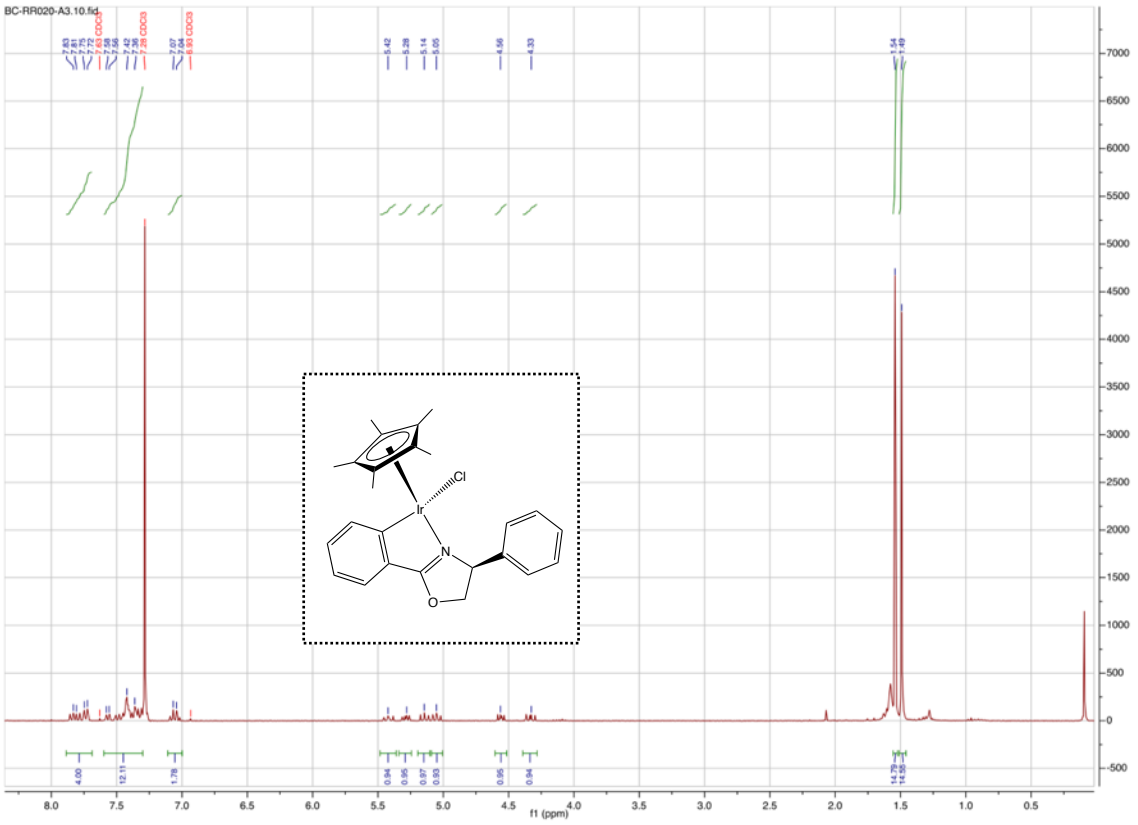

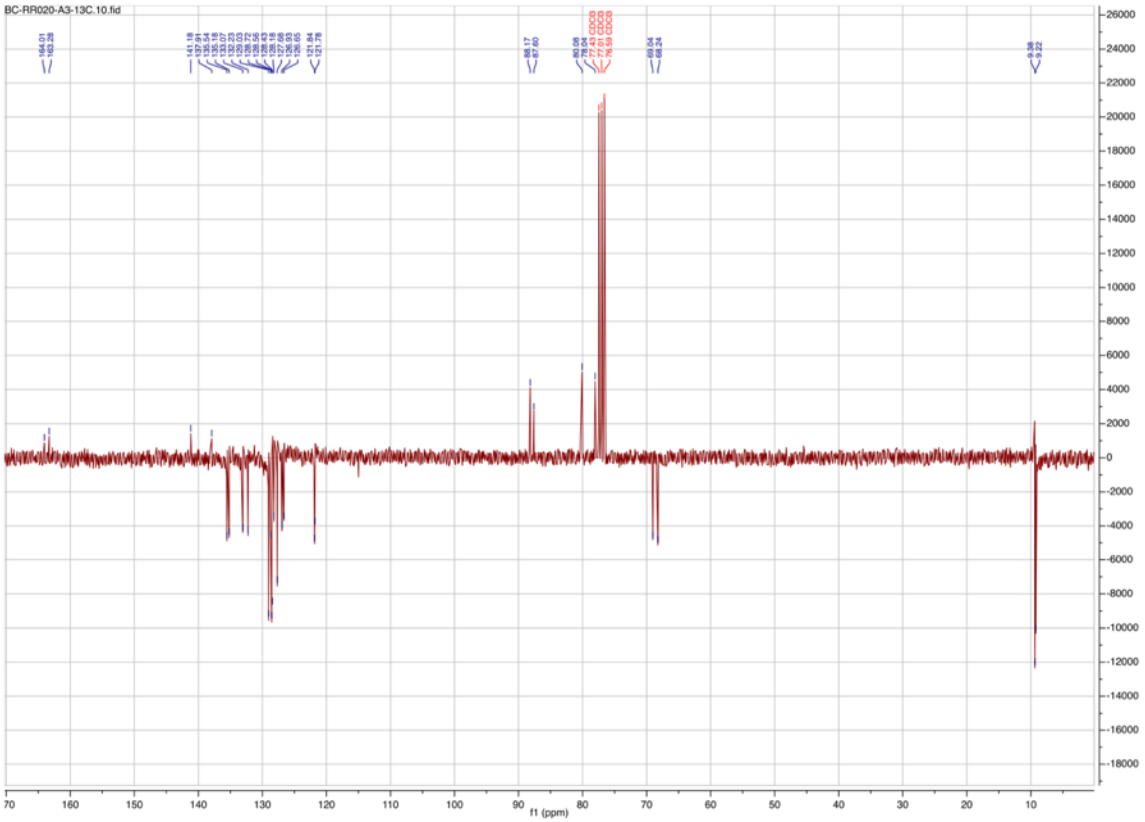

Ir10